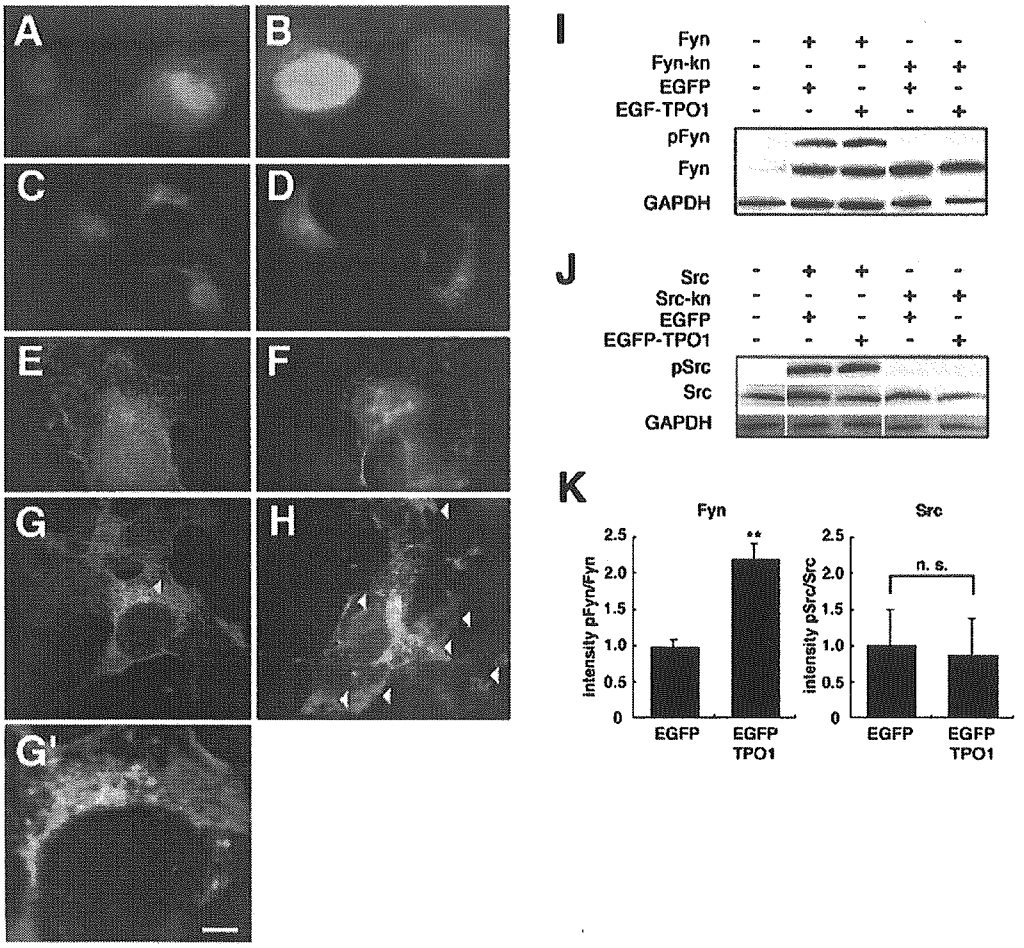


**Fig. 7 – TPO1 promotes autophosphorylation of Fyn tyrosine kinase. (A–H) Immunocytochemical analyses of TPO1, Fyn and phosphorylated Fyn expression patterns. COS7 cells were cotransfected with pEGFP (A, B, E and F) or pEGFP-TPO1 (C, D, G and H) together with wild-type Fyn (E–G) or mock (A–D) expression vectors. After transient expression (for 24 hr), fixed cells were stained with anti-Fyn (A, C, E and G) or anti-phospho-Src family (B, D, F and H), and staining was visualized using red fluorescence. EGFP and EGFP-TPO1 are distributed in uniform (A, B, E and F) and in Golgi-like patterns (C, D, G and H), respectively. G′ is a magnified image derived from G. Arrows in G′ indicate overlapping signals (yellow). Images were obtained using a cooled CCD camera. Scale bar (A) = 10 μm, Scale bar (G′) = 5 μm. (I) Immunoblot analysis of phosphorylated Fyn. COS7 cells were cotransfected with pEGFP or pEGFP-TPO1 together with wild-type Fyn (wt) or kinase-negative (kn) Fyn expression vectors. Cell lysates were prepared and analyzed by immunoblotting with anti-phospho-Src family, anti-Fyn, or anti-GAPDH, as indicated. (J) Immunoblot analysis of phosphorylated Src. COS7 cells were cotransfected with pEGFP or pEGFP-TPO1 together with wild-type Src (wt) or kinase-negative (kn) Src expression vectors. Cell lysates were prepared and analyzed by immunoblotting with anti-phospho-Src family, anti-c-Src, or anti-GAPDH as indicated. (K) Relative Fyn and Src phosphorylation levels (phosphorylated Fyn or Src signal/total Fyn or Src signal/GAPDH signal) in pEGFP-TPO1-transfected cells and in pEGFP-transfected cells. Each bar represents the mean ± SEM ($n = 3$). $^{**}P < 0.01$.**

(Simons and Ikonen, 1997; Verkade and Simons, 1997). Thus, TPO1 palmitoylation may be required for interactions with signal transduction molecules, including Fyn kinase.

In this study, we found that TPO1 promotes the autophosphorylation of Fyn kinase. Several lines of evidence suggest that Fyn is essential for myelination. Fyn-deficient mice exhibit abnormal myelination and loss of myelin content, and Fyn activity has been suggested to directly regulate MBP gene transcription (Umemori et al., 1999). In vitro experiments with cultured OLs have shown that Fyn is required for OL development and morphological differentiation (Osterhout et al., 1999; Sperber and McMorris, 2001; Klein et al., 2002; Colognato et al., 2004; Liang et al., 2004). Fyn is a non-receptor-type tyrosine kinase, coupling multiple cell surface membrane proteins to transduce extracellular signals. The cell surface membrane proteins, MAG, F3, NCAM120, FcRγ and integrin act as receptors coupled with Fyn in myelinating cells (Umemori et al., 1994; Kramer et al., 1999; Klein et al., 2002; Nakahara et al., 2003; Colognato et al., 2004; Liang et al., 2004), and these receptors have been proposed to mediate the cell–cell interactions/signaling necessary for myelin formation and maintenance. Although we demonstrated that cross linking of

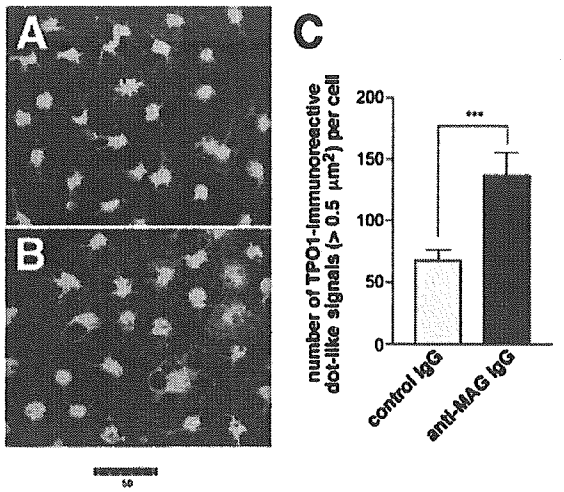


**Fig. 8 – MAG cross-linking induces an increase in dot-like signals of TPO1 in immature OLs. (A, B) Immature OLs were incubated with control mouse IgG (A) or anti-mouse MAG IgG (B), followed by anti-mouse IgG. Cells were then immunostained with anti-TPO1. Images were obtained by confocal microscopy. Scale bar = 50 μm. (C) Quantification of the number of TPO1-immunoreactive dot-like signals (>0.5 μm²) per cell in the control IgG-treated or anti-MAG IgG-treated immature OLs. Each bar represents the mean ± SEM (n = 21 cells in each case). ***$P < 0.001$.**

cell surface MAG altered the localization of TPO1 in OL-lineage cells (Fig. 8), it remains to be determined whether TPO1 is expressed at the cell surface and whether it directly interacts with Fyn and Fyn-associated receptors. TPO1 may function to regulate receptor-mediated signal that evoke Fyn kinase activation during myelination. Together with the proposed functions of AIGP1 in axonal damage and subsequent neuronal cell death (Aoki et al., 2002), a functional link between the AIGP family members may exist in neuron-OL/Schwann cell interactions. The elucidation of such a molecular link may be useful in clinical studies directed toward the prevention and treatment of myelin diseases.

## 4. Experimental procedures

### 4.1. *Antibodies*

The following monoclonal and polyclonal antibodies were used in this study: Monoclonal antibodies. RAN-2 (Bartlett et al., 1981), A2B5 (Eisenbarth et al., 1979), O4, anti-MAG, rat anti-MBP and anti-galactocerebroside (GalC) and anti-glyceraldehydes-3-phosphate dehydrogenase (GAPDH) (Chemicon International, Temecula, CA), Cy3-conjugated anti-glial fibrillary acidic protein (GFAP) (Sigma, St. Louis, MO), anti-microtubule-associated protein-2 (Map-2) (Leinco Technologies, St. Louis, MO), anti-KDEL and anti-lysosome-associated membrane glycoprotein-1 (Lamp-1) (Stressgen Biotechnologies, Victoria, BC), anti-GM130, anti-early endosome antigen1 (EEA1) and anti-Fyn (Transduction Laboratories, Lexington, KY), anti-Rab3a antibodies (Synaptic Systems, Göttingen, Germany). Polyclonal antibodies. Anti-c-Src (SRC 2) (Santa Cruz Biotechnology, Santa Cruz, CA) and anti-phospho-Src family (Tyr416) antibodies (Cell Signaling Technology, Beverly, MA). All Alexa Fluor fluorescein secondary antibody conjugates were purchased from Molecular Probes (Eugene, OR). Goat anti-mouse IgG for MAG cross-link was obtained from SouthernBiotech (Birmingham, AL).

### 4.2. *SYBR green-based real-time quantitative RT-PCR*

SYBR green-based real-time quantitative reverse transcription-polymerase chain reaction (RT-PCR) was performed as previously described (Wong et al., 2000; Aoki et al., 2002). Total RNA was isolated from whole brains of C57BL/6J mice at embryonic day 14 (E14), and postnatal days 1 (P1), 5, 10, 15, 20, 25 and 8 weeks. Total RNA (1 μg) was treated with DNase I and converted to cDNA using Superscript reverse transcriptase (Invitrogen, Carlsbad, CA) and random hexamer primers. Real-time RT-PCR was performed in a total reaction volume of 25 μl using an Applied Biosystems (Foster City, CA) 7700 Sequence Detection System. The following primer pairs were used: 5′-TGTTGGAGGCTTGGCTTTGA-3′ (nt 642–661; forward) and 5′-ACCAGAGAGATTAGCACGCA-3′ (nt 733–752; reverse) for amplification of the TPO1 gene (GenBank accession no. AB029501); 5′-ATTCCTCTTCCTGCAGCACAG-3′ (nt 581–601; forward) and 5′-TGTTATCTTCCAGCAGGGCAC-3′ (nt 669–689; reverse) for amplification of the MOG gene (GenBank accession no. U64572); 5′-TCCTTCTGGTCCAGTGAATGG-3′ (nt 321–341; forward) and 5′-CGATGTAAGGTTGTCCCTTGG-3′ (nt 418–438; reverse) for amplification of the P0 gene (GenBank accession no. NM_008623); and 5′-AGAGACAACATTGGCATGGCT-3′ (nt 1282–1302; forward) and 5′-AATCCTGATCAAAAGCGCG-3′ (nt 1379–1498; reverse) for amplification of the β-actin gene (GenBank accession no. NM_007393) (Aoki et al., 2002). Control experiments (melting temperature analysis and agarose gel electrophoresis of PCR products) established that the signal for each amplicon was derived from cDNA and not from primer–dimers. The quantitative RT-PCR method (User Bulletin #2, Applied Biosystems) was modified to establish an expression level index for mRNA (Aoki et al., 2002), and all data were normalized to the SYBR green signal for β-actin amplicon.

### 4.3. *Antibody production*

Polyclonal antibodies against TPO1 (ABEP06 and ABEP05) were obtained by immunizing rabbits with the synthetic epitope peptide 06 (EP06) (VMKQVKDHIPSFE; aa 58–70 in mouse TPO1; GenBank accession no. AB029501) or epitope peptide 05 (EP05) (SDALQSRYGAPE; aa 339–350 in mouse TPO1). Rabbits were immunized with each peptide coupled to keyhole limpet hemocyanin in complete adjuvant four times at 2-week intervals. The resulting antisera were affinity-purified on EP05- or EP06-coupled peptide columns using a SulfoLink kit (Pierce, Rockford, IL) according to the manufacturer's protocol.

### 4.4. *Western blot analysis of TPO1*

Western Blotting was performed as described previously (Aoki et al., 2002), with minor modifications. Mouse cortical OLs cultured for 3 days were suspended in phosphate-buffered saline (PBS) containing complete protease inhibitor mixture (Roche, Lewes, East Sussex, UK) and lysed on ice using a Handy Sonic model UR-20P (power level 3–4; TOMY, Tokyo, Japan). To separate membrane and soluble fractions, the lysates were centrifuged at 12,000×g for 30 min at 4 °C. Protein concentration was determined using a protein assay kit (Bio-Rad, Hercules, CA), and equivalent amounts of soluble and membrane proteins from both fractions were resolved by electrophoresis on a 10–20% gradient sodium dodecyl sulfate-polyacrylamide gel (SDS-PAGE). The resolved proteins were then transferred to a PVDF membrane (Bio-Rad) using a semi-dry electroblotter (Bio-Rad). The membrane was blocked by incubation in 1% bovine serum albumin (BSA)/PBS containing 0.1% (v/v) Tween-20 for 1 hr at room temperature (RT). ABEP05 (1 μg/ml) or negative control normal rabbit IgG (1 μg/ml) was used as a primary antibody, and horseradish peroxidase (HRP)-conjugated

anti-rabbit IgG (H+L) (Dako, Carpinteria, CA) was used as secondary antibody. Immunoreactive bands were detected using the Super-signal Substrate System (Pierce) according to the manufacturer's instructions. The specificity of the TPO1 antibodies was evaluated using the following methods: (1) COS7 cells transfected with a C-terminal Myc-tagged mouse TPO1 expression construct were immunostained with an affinity-purified antibody against EP05 or 06 (ABEP05 or ABEP06). Staining showed Golgi-localized small puncta and completely overlapped that of anti-Myc (data not shown). No signal was observed in COS7 cells transfected with a mock construct (data not shown). (2) Affinity-purified ABEP05 and 06 antibodies were pre-incubated with 100-fold excess of EP05 and EP06 or with an unrelated peptide as a negative control. TPO1 staining was abolished by pre-absorption with the corresponding antigens (data not shown), and incubation with the negative control peptide had no effect on the staining pattern (data not shown). (3) As a negative control, cells or tissue sections were stained with rabbit IgG (Dako) at the same concentrations used in immunohistochemical experiments (Fig. 2Cd). No signal was observed. (4) Staining with anti-AIGP1 (a member of the AIGP protein family) or anti-TPO1 showed no myelin (Aoki et al., 2002) or neuronal staining (Figs. 3Ca, b and c), respectively, indicating no cross reactivity of the antibodies.

### 4.5. *Genotyping of trembler-Ncnp mice by genomic DNA PCR*

Genotyping of trembler-Ncnp mice was performed as described previously (Suh et al., 1997; Sakai et al., 1999). The two forward primers, 5′-TCAGGGACAGTACCAGAGCTCA-3′ and 5′-CCGTATT-TCTCGATCACACAC-3′, and the reverse primer, 5′-GAGCTAGT-TAGCTGCTGGACA-3′, were used for genotyping of wild-type, and trembler-Ncnp heterozygotes and homozygotes. The primer set can simultaneously amplify two different fragments to identify trembler-Ncnp and wild-type genotypes. PCR was performed using the GeneAmp PCR system 9700 (Applied Biosystems). Genomic DNA was pre-heated at 94 °C for 3 min, followed by 30 cycles of PCR (denaturation at 94 °C for 15 s, annealing at 57 °C for 2 min and polymerization at 72 °C for 2 min). After a final extension at 72 °C for 10 min, PCR products were analyzed on 2% agarose gels.

### 4.6. *Immunohistochemistry*

C57BL/6J mice were anesthetized and perfused with 4% paraformaldehyde (PFA). The brains were removed and post-fixed overnight, cryoprotected in 30% sucrose in PBS, and frozen in dry ice. Sections (20 μm) were cut with a Frigocut 2800 cryostat (Reichert-Jung, Wien, Austria), placed onto APS-coated glass slides, fixed with 4% PFA, washed three times with PBS, permeabilized with 0.1% (v/v) Triton X-100/PBS for 5 min and finally washed three times with PBS. Fixed sections were incubated for 30 min with 5% goat serum (Nichirei, Tokyo, Japan) in PBS. Sections were incubated overnight at 4 °C with diluted primary polyclonal and/or monoclonal antibody in 1% goat serum/PBS. These sections were incubated for 1 hr with diluted Alexa Fluor fluorescein-conjugated secondary antibody (Molecular Probes) and washed several times with PBS. Antibody dilutions were as follows: ABP05, 1 μg/ml; anti-Map2, 1:200; anti-GFAP, 1:200; O4, 1:50 and anti-MBP, 1:50. All secondary antibodies were used at a 1:200 dilution. Images of stained cells were obtained using a FluoView confocal microscope system (Olympus, Tokyo, Japan). For diaminobenzidine tetrahydrochloride (DAB) staining, paraffin sections (5 μm thick) of sciatic nerve and cerebellum from trembler-Ncnp and wild-type mice were prepared and stained with primary antibody. HRP-conjugated anti-rabbit antibody (Dako) was used as secondary antibody, and signals were visualized with DAB solution containing 0.3% $H_2O_2$ in PBS. Images were obtained with a CCD camera (HC-2500; Fujifilm, Kanagawa, Japan).

### 4.7. *Embryonic neuroepithelial cell culture*

Embryonic neuroepithelial cells were prepared from E14 mouse telencephalon as previously described (Nakashima et al., 1999). Cells were mechanically dissociated by trituration and plated on dishes ($1.0\times10^4$ cells per dish; ϕ10 cm) coated with 15 μg/ml poly-L-ornithine (Sigma) and 1 μg/ml fibronectin (Asahi technoglass, Tokyo, Japan). Initially, plated cells were expanded for 4 days in B27-supplemented Neurobasal medium (Invitrogen) containing 10 ng/ml basic fibroblast growth factor (Peprotech, Rocky Hill, NJ) on dishes coated with poly-L-ornithine and fibronectin. Cells were then detached and replated on 4-well chamber slides (Nalgene Nunc International, Rochester, NY) at $5.0\times10^4$ cells per well for immunofluorescence staining.

### 4.8. *Immunopanning purification and cultivation of rat optic nerve oligodendrocyte precursor cells (OPCs)*

Rat optic nerve OPCs were prepared from optic nerves of P7 rats and purified by the immunopanning method (Barres et al., 1992) with minor modifications. Dissected optic nerves were mechanically dissociated and incubated for 75 min in a solution of 32 U/ml papain (Worthington, Freehold, NJ), 0.4 mg/ml L-cysteine (Sigma) and 0.004% DNase I (Sigma) in minimum essential medium (Invitrogen). Low ovomucoid trypsin inhibitor solution was added to stop the reaction. After centrifugation, the supernatant was removed and the cells suspended in high ovomucoid trypsin inhibitor solution. Cell aggregates were mechanically disrupted to single cells by pipetting, and then the cells were passed through a nylon mesh (20 μm pore size). After centrifugation, cells were suspended in L15/BSA medium (Invitrogen). The OPCs were purified by incubation of the cell suspension on a Ran2-coated dish for 20 min to remove type-1 astrocytes and microglia and then on an anti-GalC-coated dish for 30 min to remove mature OLs. Finally, cells were allowed to attach onto A2B5-coated dishes for 30 min. OPCs were detached from A2B5 dishes via trypsinization and replated on poly-D-lysine-coated flasks. OPCs were cultured in B-S medium: Dulbecco's modified Eagle' medium (DMEM) containing 10 μg/ml insulin, 5 ng/ml NT-3 (Peprotech), 100 μg/ml human transferrin, 100 μg/ml BSA, 60 ng/ml progesterone, 40 ng/ml sodium selenite, 63 μg/ml N-acetyl-cysteine, 16 μg/ml putrescine, 10 ng/ml D-biotin, 5 μM forskolin and penicillin–streptomycin–glutamine (Invitrogen) (other ingredients from Sigma). Human PDGF-AA (10 ng/ml, Peprotech) was added for proliferation of OPCs and then removed to induce differentiation of mature OLs.

### 4.9. *Immunocytochemistry*

Cultured cells were grown on poly-D-lysine-coated dishes for immunofluorescence staining. All incubations and washes were performed at RT. Cells were fixed with 4% PFA and then washed three times with PBS. Fixed cells were incubated for 30 min in blocking solution (1% BSA, 0.1% (v/v) Triton X-100, and 20% goat serum in 0.1 M PBS) and washed with PBS. Cells were incubated with diluted primary polyclonal and/or monoclonal antibody in the incubation buffer (1% BSA and 0.1% (v/v) Triton X-100 in PBS). Cells were then incubated for 30 min with diluted secondary antibody conjugated to Alexa Fluor fluorescein (Molecular Probes) and washed with PBS. Antibody concentrations and dilutions were as follows: ABEP05, 5 μg/ml; A2B5, 1:500; O4, 1:200; anti-GalC, 1:200; anti-MBP, 1:200; anti-Fyn, 1:200; and anti-phospho-Src family, 1:100. All secondary antibodies were diluted 1:200. Images were obtained using epifluorescence microscopy (Olympus IX70) or confocal microscopy (Olympus FluoView).

### 4.10. *Expression constructs*

To construct a TPO1-enhanced green fluorescent protein (EGFP) expression plasmid, a 1.4-kbp cDNA fragment of pCI-neo mouse

TPO1 (Aoki et al., 2002) was ligated between the *Xho*I and *Eco*RI sites of pEGFP-C1 (Invitrogen). Wild-type Fyn, kinase-negative Fyn (K299M), wild-type Src and kinase-negative Src (K299M) expression vectors (Takeuchi et al., 1993) were kindly provided by Dr. T. Yamamoto (Division of Oncology, Department of Cancer Biology, Institute of Medical Science University of Tokyo, Japan).

### 4.11. *Analyses of autophosphorylation of Fyn and Src*

COS7 cells were plated in 6-well dishes at a density of $4.0 \times 10^4$ cells/$cm^2$, cultured for 24 hr, and transfected with DNA using Lipofectamine (Invitrogen). After 6 hr, the medium was replaced with 0.1% fetal bovine serum/DMEM. At 18 hr post-transfection, the cells were washed twice with PBS and solubilized with RIPA buffer (20 mM Tris–HCl, pH 7.4, 150 mM NaCl, 1 mM EDTA, 1% (v/v) Nonidet P-40, 10% (v/v) glycerol, 0.1% SDS, 0.5% deoxycholate, 1 mM sodium orthovanadate and complete protease inhibitor mixture) for 20 min on ice. The lysate was centrifuged at 12,000×*g* for 30 min at 4 °C. Proteins were separated by SDS-PAGE and transferred electrophoretically to PVDF membranes. The membranes were blocked with 3% non-fat milk in Tris-buffered saline containing 0.1% (v/v) Tween-20 (T-TBS) for 1 hr at RT, incubated with primary antibodies in 3% BSA/T-TBS overnight at 4 °C, washed with T-TBS, incubated with HRP-conjugated secondary antibodies for 1 hr at RT, and washed with T-TBS. Antibodies were diluted as follows: anti-Fyn, 1:250; anti-c-Src, 1:50; anti-phospho-Src family, 1:1000; and anti-GAPDH, 1:300. Anti-mouse or anti-rabbit IgG (H+L) conjugated with HRP was used as secondary antibody. Immunoreactive bands were detected using the Supersignal Substrate System (Pierce) according to the manufacturer's instructions. The intensity of bands was quantified with FluorChem ver. 2.0 software (Alpha Innotech, San Leandro, CA).

### 4.12. *MAG cross-linking*

The MAG cross-linking experiment was performed as described (Marta et al., 2004) with minor modifications. Briefly, immature OLs were prepared by treatment with differentiation medium (B–S medium lacking PDGF-AA). The immature OLs were washed with DMEM and incubated for 15 min at 37 °C with monoclonal anti-MAG IgG (2.5 μg/ml) or control mouse IgG (2.5 μg/ml) diluted in B–S medium. The anti-MAG IgG or control IgG was washed out with DMEM, and the OLs were incubated with goat anti-mouse IgG (10 μg/ml) for 30 min at 37 °C and then fixed for immunocytochemistry.

## Acknowledgments

We thank for Dr. Y. Tokumoto for technical advice and helpful suggestions. This work was supported by Grants-in-Aid for Scientific Research from the Ministry of Health, Labour and Welfare of Japan, Grants-in-Aid for Scientific Research from the Ministry of Education, Culture, Sports, science and Technology of Japan, a grant from the Organization for Pharmaceutical Safety and Research, a grant from Japan Science and Technology Cooperation, and new energy and industrial technology development organization (NEDO).

## REFERENCES

Aoki, S., Su, Q., Li, H., Nishikawa, K., Ayukawa, K., Hara, Y., Namikawa, K., Kiryu-Seo, S., Kiyama, H., Wada, K., 2002. Identification of an axotomy-induced glycosylated protein, AIGP1, possibly involved in cell death triggered by endoplasmic reticulum-Golgi stress. J. Neurosci. 22, 10751–10760.

Barres, B.A., Hart, I.K., Coles, H.S., Burne, J.F., Voyvodic, J.T., Richardson, W.D., Raff, M.C., 1992. Cell death and control of cell survival in the oligodendrocyte lineage. Cell 70, 31–46.

Bartlett, P.F., Noble, M.D., Pruss, R.M., Raff, M.C., Rattray, S., Williams, C.A., 1981. Rat neural antigen-2 (RAN-2): a cell surface antigen on astrocytes, ependymal cells. Muller cells and lepto-meninges defined by a monoclonal antibody. Brain Res. 204, 339–351.

Baumann, N., Pham-Dinh, D., 2001. Biology of oligodendrocyte and myelin in the mammalian central nervous system. Physiol. Rev. 81, 871–927.

Chen, J.W., Murphy, T.L., Willingham, M.C., Pastan, I., August, J.T., 1985. Identification of two lysosomal membrane glycoproteins. J. Cell Biol. 101, 85–95.

Colognato, H., Ramachandrappa, S., Olsen, I.M., Ffrench-Constant, C., 2004. Integrins direct Src family kinases to regulate distinct phases of oligodendrocyte development. J. Cell Biol. 167, 365–375.

Eisenbarth, G.S., Walsh, F.S., Nirenberg, M., 1979. Monoclonal antibody to a plasma membrane antigen of neurons. Proc. Natl. Acad. Sci. U. S. A. 76, 4913–4917.

Fukuda, M., Kanno, E., Saegusa, C., Ogata, Y., Kuroda, T.S., 2002. Slp4-a/granuphilin-a regulates dense-core vesicle exocytosis in PC12 cells. J. Biol. Chem. 277, 39673–39678.

Grossman, T.R., Luque, J.M., Nelson, N., 2000. Identification of a ubiquitous family of membrane proteins and their expression in mouse brain. J. Exp. Biol. 203 (Pt. 3), 447–457.

Han, K.K., Martinage, A., 1992. Possible relationship between coding recognition amino acid sequence motif or residue(s) and post-translational chemical modification of proteins. Int. J. Biochem. 24, 1349–1363.

Hirayama, A., Oka, A., Ito, M., Tanaka, F., Okoshi, Y., Takashima, S., 2003. Myelin transcription factor 1 (MyT1) immunoreactivity in infants with periventricular leukomalacia. Brain Res. Dev. Brain Res. 140, 85–92.

Kidd, G.J., Hauer, P.E., Trapp, B.D., 1990. Axons modulate myelin protein messenger RNA levels during central nervous system myelination in vivo. J. Neurosci. Res. 26, 409–418.

Klein, C., Kramer, E.M., Cardine, A.M., Schraven, B., Brandt, R., Trotter, J., 2002. Process outgrowth of oligodendrocytes is promoted by interaction of fyn kinase with the cytoskeletal protein tau. J. Neurosci. 22, 698–707.

Klugmann, M., Schwab, M.H., Puhlhofer, A., Schneider, A., Zimmermann, F., Griffiths, I.R., Nave, K.A., 1997. Assembly of CNS myelin in the absence of proteolipid protein. Neuron 18, 59–70.

Koegl, M., Zlatkine, P., Ley, S.C., Courtneidge, S.A., Magee, A.I., 1994. Palmitoylation of multiple Src-family kinases at a homologous N-terminal motif. Biochem. J. 303 (Pt. 3), 749–753.

Kramer, E.M., Klein, C., Koch, T., Boytinck, M., Trotter, J., 1999. Compartmentation of Fyn kinase with glycosylphosphatidylinositol-anchored molecules in oligodendrocytes facilitates kinase activation during myelination. J. Biol. Chem. 274, 29042–29049.

Krueger, W.H., Gonye, G.E., Madison, D.L., Murray, K.E., Kumar, M., Spoerel, N., Pfeiffer, S.E., 1997. TPO1, a member of a novel protein family, is developmentally regulated in cultured oligodendrocytes. J. Neurochem. 69, 1343–1355.

Kyte, J., Doolittle, R.F., 1982. A simple method for displaying the hydropathic character of a protein. J. Mol. Biol. 157, 105–132.

Li, C., Tropak, M.B., Gerlai, R., Clapoff, S., Abramow-Newerly, W., Trapp, B., Peterson, A., Roder, J., 1994. Myelination in the absence of myelin-associated glycoprotein. Nature 369, 747–750.

Liang, X., Draghi, N.A., Resh, M.D., 2004. Signaling from integrins to Fyn to Rho family GTPases regulates morphologic differentiation of oligodendrocytes. J. Neurosci. 24, 7140–7149.

Lupski, J.R., de Oca-Luna, R.M., Slaugenhaupt, S., Pentao, L., Guzzetta, V., Trask, B.J., Saucedo-Cardenas, O., Barker, D.F., Killian, J.M., Garcia, C.A., et al., 1991. DNA duplication associated with Charcot–Marie–Tooth disease type 1A. Cell 66, 219–232.

Macklin, W.B., Weill, C.L., Deininger, P.L., 1986. Expression of myelin proteolipid and basic protein mRNAs in cultured cells. J. Neurosci. Res. 16, 203–217.

Marta, C.B., Taylor, C.M., Cheng, S., Quarles, R.H., Bansal, R., Pfeiffer, S.E., 2004. Myelin associated glycoprotein cross-linking triggers its partitioning into lipid rafts, specific signaling events and cytoskeletal rearrangements in oligodendrocytes. Neuron Glia Biology 1, 35–46.

Matsuda, Y., Koito, H., Yamamoto, H., 1997. Induction of myelin-associated glycoprotein expression through neuron-oligodendrocyte contact. Brain Res. Dev. Brain Res. 100, 110–116.

Mu, F.T., Callaghan, J.M., Steele-Mortimer, O., Stenmark, H., Parton, R.G., Campbell, P.L., McCluskey, J., Yeo, J.P., Tock, E.P., Toh, B.H., 1995. EEA1, an early endosome-associated protein. EEA1 is a conserved alpha-helical peripheral membrane protein flanked by cysteine "fingers" and contains a calmodulin-binding IQ motif. J. Biol. Chem. 270, 13503–13511.

Nakahara, J., Tan-Takeuchi, K., Seiwa, C., Gotoh, M., Kaifu, T., Ujike, A., Inui, M., Yagi, T., Ogawa, M., Aiso, S., Takai, T., Asou, H., 2003. Signaling via immunoglobulin Fc receptors induces oligodendrocyte precursor cell differentiation. Dev. Cell 4, 841–852.

Nakamura, N., Rabouille, C., Watson, R., Nilsson, T., Hui, N., Slusarewicz, P., Kreis, T.E., Warren, G., 1995. Characterization of a cis-Golgi matrix protein, GM130. J. Cell Biol. 131, 1715–1726.

Nakashima, K., Yanagisawa, M., Arakawa, H., Kimura, N., Hisatsune, T., Kawabata, M., Miyazono, K., Taga, T., 1999. Synergistic signaling in fetal brain by STAT3–Smad1 complex bridged by p300. Science 284, 479–482.

Osterhout, D.J., Wolven, A., Wolf, R.M., Resh, M.D., Chao, M.V., 1999. Morphological differentiation of oligodendrocytes requires activation of Fyn tyrosine kinase. J. Cell Biol. 145, 1209–1218.

Sakai, Y., Nakabayashi, O., Kikuchi, T., Wada, K., 1999. Identification of break points in mutated PMP22 gene in a new Trembler (Tr-Ncnp) mouse. Neuroscience 88, 989–991.

Sakamoto, Y., Kitamura, K., Yoshimura, K., Nishijima, T., Uyemura, K., 1987. Complete amino acid sequence of PO protein in bovine peripheral nerve myelin. J. Biol. Chem. 262, 4208–4214.

Schneider, A., Lander, H., Schulz, G., Wolburg, H., Nave, K.A., Schulz, J.B., Simons, M., 2005. Palmitoylation is a sorting determinant for transport to the myelin membrane. J. Cell Sci. 118, 2415–2423.

Scolding, N.J., Frith, S., Linington, C., Morgan, B.P., Campbell, A.K., Compston, D.A., 1989. Myelin-oligodendrocyte glycoprotein (MOG) is a surface marker of oligodendrocyte maturation. J. Neuroimmunol. 22, 169–176.

Shenoy-Scaria, A.M., Gauen, L.K., Kwong, J., Shaw, A.S., Lublin, D.M., 1993. Palmitylation of an amino-terminal cysteine motif of protein tyrosine kinases p56lck and p59fyn mediates interaction with glycosyl-phosphatidylinositol-anchored proteins. Mol. Cell. Biol. 13, 6385–6392.

Shy, M.E., Garbern, J.Y., Kamholz, J., 2002. Hereditary motor and sensory neuropathies: a biological perspective. Lancet Neurol. 1, 110–118.

Simons, K., Ikonen, E., 1997. Functional rafts in cell membranes. Nature 387, 569–572.

Sperber, B.R., McMorris, F.A., 2001. Fyn tyrosine kinase regulates oligodendroglial cell development but is not required for morphological differentiation of oligodendrocytes. J. Neurosci. Res. 63, 303–312.

Suh, J.G., Ichihara, N., Saigoh, K., Nakabayashi, O., Yamanishi, T., Tanaka, K., Wada, K., Kikuchi, T., 1997. An in-frame deletion in peripheral myelin protein-22 gene causes hypomyelination and cell death of the Schwann cells in the new Trembler mutant mice. Neuroscience 79, 735–744.

Suter, U., Welcher, A.A., Ozcelik, T., Snipes, G.J., Kosaras, B., Francke, U., Billings-Gagliardi, S., Sidman, R.L., Shooter, E.M., 1992. Trembler mouse carries a point mutation in a myelin gene. Nature 356, 241–244.

Takeuchi, M., Kuramochi, S., Fusaki, N., Nada, S., Kawamura-Tsuzuku, J., Matsuda, S., Semba, K., Toyoshima, K., Okada, M., Yamamoto, T., 1993. Functional and physical interaction of protein-tyrosine kinases Fyn and Csk in the T-cell signaling system. J. Biol. Chem. 268, 27413–27419.

Umemori, H., Sato, S., Yagi, T., Aizawa, S., Yamamoto, T., 1994. Initial events of myelination involve Fyn tyrosine kinase signalling. Nature 367, 572–576.

Umemori, H., Kadowaki, Y., Hirosawa, K., Yoshida, Y., Hironaka, K., Okano, H., Yamamoto, T., 1999. Stimulation of myelin basic protein gene transcription by Fyn tyrosine kinase for myelination. J. Neurosci. 19, 1393–1397.

Vallat, J.M., Sindou, P., Garbay, B., Preux, P.M., Anani, T., Richard, L., Diot, M., 1999. Expression of myelin proteins in the adult heterozygous Trembler mouse. Acta Neuropathol. (Berl.) 98, 281–287.

Vaux, D., Tooze, J., Fuller, S., 1990. Identification by anti-idiotype antibodies of an intracellular membrane protein that recognizes a mammalian endoplasmic reticulum retention signal. Nature 345, 495–502.

Verkade, P., Simons, K., 1997. Robert Feulgen Lecture 1997. Lipid microdomains and membrane trafficking in mammalian cells. Histochem. Cell Biol. 108, 211–220.

Weissert, R., Wallstrom, E., Storch, M.K., Stefferl, A., Lorentzen, J., Lassmann, H., Linington, C., Olsson, T., 1998. MHC haplotype-dependent regulation of MOG-induced EAE in rats. J. Clin. Invest. 102, 1265–1273.

Wolven, A., Okamura, H., Rosenblatt, Y., Resh, M.D., 1997. Palmitoylation of p59fyn is reversible and sufficient for plasma membrane association. Mol. Biol. Cell 8, 1159–1173.

Wong, M.H., Saam, J.R., Stappenbeck, T.S., Rexer, C.H., Gordon, J.I., 2000. Genetic mosaic analysis based on Cre recombinase and navigated laser capture microdissection. Proc. Natl. Acad. Sci. U. S. A. 97, 12601–12606.

# Pax6 is required for production and maintenance of progenitor cells in postnatal hippocampal neurogenesis

**Motoko Maekawa[1,3], Noriko Takashima[1,2], Yoko Arai[1], Tadashi Nomura[1], Kaoru Inokuchi[2], Shigeki Yuasa[3] and Noriko Osumi[1,4,*]**

[1]*Division of Developmental Neuroscience, Center for Translational and Advanced Animal Research (CTAAR), Tohoku University School of Medicine, 2-1 Seiryo-machi, Aoba-ku, Sendai 980-8575, Japan*

[2]*Mitsubishi Kagaku Institute of Life Sciences (MITILS), Minamiooya 11, Machida, Tokyo 194-8511, Japan*

[3]*Department of Ultrastructural Research, National Institute of Neuroscience, National Center of Neurology and Psychiatry, 4-1-1 Ogawahigashi-machi, Kodaira, Tokyo 187-8502, Japan*

[4]*CREST, Japan Science and Technology Corporation (JST), 4-1-8 Honmachi, Kawaguchi, 332-0012, Japan*

**Neurogenesis is crucial for brain formation and continues to take place in certain regions of the postnatal brain including the subgranular zone (SGZ) of the hippocampal dentate gyrus (DG). Pax6 transcription factor is a key player for patterning the brain and promoting embryonic neurogenesis, and is also expressed in the SGZ. In the DG of wild-type rats, more than 90% of total BrdU-incorporated cells expressed Pax6 at 30 min time point after BrdU injection. Moreover, approximately 60% of Pax6$^+$ cells in the SGZ exhibited as GFAP$^+$ cells with a radial glial phenotype and about 30% of Pax6$^+$ cells exhibited as PSA-NCAM$^+$ cells in clusters. From BrdU labeling for 3 days, we found that cell proliferation was 30% decreased at postnatal stages in *Pax6*-deficient *rSey$^2$*/+ rat. BrdU pulse/chase experiments combined with marker staining revealed that PSA-NCAM$^+$ late progenitor cells increased at the expense of GFAP$^+$ early progenitors in *rSey$^2$*/+ rat. Furthermore, expression of Wnt ligands in the SGZ was markedly reduced in *rSey$^2$*/+ rat. Taken all together, an appropriate dosage of Pax6 is essential for production and maintenance of the GFAP$^+$ early progenitor cells in the postnatal hippocampal neurogenesis.**

## Introduction

Neurogenesis depends on a specific population of cells termed 'neural stem/progenitor cells' (we call here 'neural progenitor cells'). In the mammalian embryonic brain, neural progenitor cells take a feature of 'neuroepithelial cells' or 'matrix cells' (reviewed in Fujita 2003) while the adult brain contains islands of neural progenitor cells in the subventricular zone (SVZ) of the lateral ventricle and in the subgranular zone (SGZ) of the hippocampal dentate gyrus (DG) (Altman & Das 1965 and see reviews by Gage 2000; Alvarez-Buylla *et al.* 2002). These cells possess pluripotent differentiation potential; they can become neurons, astrocytes, or oligodendrocytes.

In hippocampal neurogenesis, dividing precursor cells give rise to daughter cells, which migrate away from the SGZ and start to differentiate into neurons (Seki & Arai 1993; Kuhn *et al.* 1996; Kempermann *et al.* 2003). Several lines of evidence have suggested that there are distinct subtypes of neural progenitor cells in the SGZ. In electron microscopy analysis, there are two types of mitotically active SGZ cells; type B cells that have ultrastructural features of astrocytes with light cytoplasm containing GFAP and multiple processes, rapidly convert into type D cells that are small electron-dense cells and GFAP negative (Seri *et al.* 2001). Another paper (Fukuda *et al.* 2003) has shown two distinct progenitor cells based on morphology, molecular expression, and electrical features: GFAP$^+$ type I cells with lower input resistance (IR) and PSA-NCAM$^+$ type II cells with higher IR. Roughly speaking, type I cells correspond to B cells, while type II cells to D cells. In this paper, we use GFAP$^+$ early progenitors and PSA-NCAM$^+$ late progenitors as clearer definition.

Although adult and embryonic neurogenesis differs in some aspects, there indeed is similarity. In the adult

*Communicated by*: Tetsuya Taga
**Correspondence*: E-mail: osumi@mail.tains.tohoku.ac.jp

DOI: 10.1111/j.1365-2443.2005.00893.x

hippocampus, GFAP$^+$ early progenitors have the appearance of radial glial cells, and not only do they produce neurons but also provide scaffolding for migration of newly born neurons (Forster *et al.* 2002). These features are quite similar to embryonic radial glial cells that constitute the ventricular zone (Gotz 2003; Tramontin *et al.* 2003). The finding that radial glia-like cells in the adult brain have stem cell properties (Doetsch *et al.* 1997, 1999; Seri *et al.* 2001) leads us to search for intrinsic molecular mechanisms that commonly govern pre- and postnatal neurogenesis.

A transcription factor Pax6 is strongly expressed during brain development in the discrete regions such as the dorsal telencephalon and the ventral hindbrain and serves as one of the key factor for patterning the central nervous system (see reviews by Osumi 2001; Simpson & Price 2002). Specific Pax6 expression is observed in the nucleus of the ventricular zone cells, which are most likely radial glial cells (Gotz 2003). In a spontaneous mutant *Small eye* (*Sey*) mouse that lacks functional Pax6, radial glial cells are less in number and show a distorted morphology, altered gene expression patterns and abnormal cell cycle characteristics (Stoykova *et al.* 1997; Gotz *et al.* 1998; Estivill-Torrus *et al.* 2002). A similar observation that less PCNA-positive cells constitute the thinner ventricular zone in *Small eye* rat mutant (*rSey*$^2$) has also been reported (Fukuda *et al.* 2000). Curiously enough, Pax6 is expressed not only in the embryonic neuroepithelium but also in the adult brain including the SGZ and the SVZ (Stoykova & Gruss 1994; Nakatomi *et al.* 2002; Hack *et al.* 2004, 2005); the above-mentioned regions which are known as the places that neurogenesis persists in adulthood. All these lines of evidences have prompted us to examine the role of Pax6 in postnatal neurogenesis.

Here, we show that Pax6-expressing cells in the SGZ of the hippocampus have a neural progenitor-like character at the molecular and the cellular levels. Detailed BrdU pulse/chase experiments have revealed that the ratio of GFAP$^+$ early progenitor cells in total BrdU$^+$ cells decreased, and instead, PSA-NCAM$^+$ late progenitors increased in the *Pax6*-deficient *rSey*$^2$/+ rat. Therefore Pax6 is necessary for the maintenance of the GFAP$^+$ early progenitor cells in the SGZ. We further searched for Pax6 downstream molecules that are relevant for the proliferation of neural progenitor cells in postnatal hippocampus, and found that expressions of Wnt ligands *Wnt7a* and *Wnt7b* and downstream effecter *Dvl1* are changed in the DG of the *rSey*$^2$/+. Our results suggest that a genetic cascade of Pax6–Wnt is critical for postnatal hippocampal neurogenesis especially at the early step.

## Results

### Pax6-positive cells express early progenitor markers

Previous studies have reported that Pax6 is expressed in discrete regions of the postnatal brain such as the cerebellum and the limbic system including the olfactory bulb, olfactory cortex, and hippocampus (Stoykova & Gruss 1994; Nakatomi *et al.* 2002; Hack *et al.* 2004). In the present study, we focused on Pax6 expression in the DG of which knowledge on adult neurogenesis has been gathered.

In the DG of the wild-type rat at 4 weeks when the architecture of the hippocampus is established, many Pax6$^+$ cells were observed in unique distribution patterns (Fig. 1A). A majority of Pax6$^+$ cells were located in the SGZ, sometimes in clusters of five to eight cells (Fig. 1A,C). A much smaller number of Pax6$^+$ cells were detectable in the hilus and molecular layer, whereas Pax6$^+$ cells were scarcely found in the granule cell layer (GCL). To elucidate the character of Pax6$^+$ cells, we performed double labeling with various markers for neural progenitor cells, neurons, and astrocytes (Fig. 1B,C). Many of Pax6$^+$ cells co-expressed GFAP, a marker for astrocytes or early progenitors marker (59.0%, 85/144 cells; Fig. 1B,C), and a majority of Pax6/GFAP double-positive cells had processes oriented radially into the GCL of the DG (Fig. 1C,C′; also see Fig. 5E). Pax6$^+$ cells also expressed neural stem cell markers nestin (34.4%, 20/58 cells) and Musashi1 (68.7%, 22/32 cells) (Fig. 1B). About a third of Pax6$^+$ cells co-expressed a late progenitor marker PSA-NCAM (31.5%, 41/130 cells) (Fig. 1B). Contrastingly, Pax6$^+$ cells scarcely expressed neuronal marker NeuN (1.9%: 12/652 cells) (Fig. 1B). These results suggest that Pax6$^+$ cells exhibited the neural progenitor cell-like character.

In immuno-electron microscopy, most of Pax6$^+$ cells had irregular contours and light cytoplasm containing a few ribosomes and glial filaments (Fig. 1D,D′), showing a character of B cell (Seri *et al.* 2001). A few Pax6$^+$ cells had smooth contours and dark scant cytoplasm negative for intermediate filaments (Fig. 1E,E′), showing a character of D cell (Seri *et al.* 2001). We sometimes observed Pax6$^+$ cells that had thinner and feeble glial filaments and scant dark cytoplasm, representing an intermediate character of B cell and D cell. These data suggest that more than half of Pax6$^+$ cells show morphologic features of the GFAP$^+$ early progenitor cells in the DG.

### Defects in the DG of *rSey*$^2$/+ rats

In order to elucidate the role of Pax6 in hippocampal neurogenesis, we first observed the DG of *Pax6*-deficient

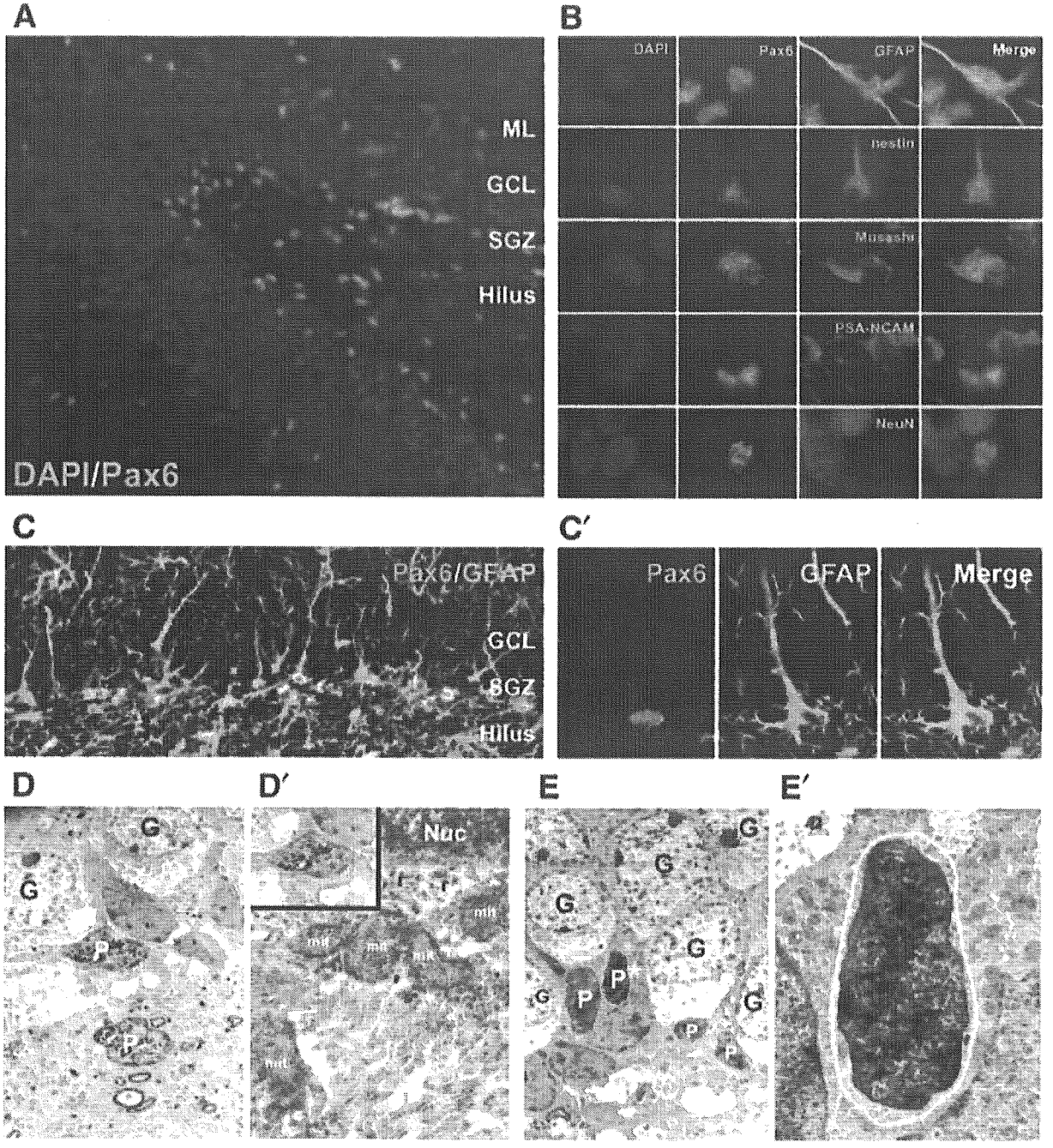


**Figure 1** Pax6$^+$ cells in the DG of the 4-week-old wild-type rat. (A) Many Pax6$^+$ cells (magenta) are observed in the subgranular zone (SGZ) and hilus. DAPI, nuclear staining; ML, molecular layer; GL, granular layer. (B) Pax6$^+$ cells co-express an early progenitor marker GFAP, neural stem cell markers nestin and Musashi1, and a late progenitor marker PSA-NCAM, but scarcely co-express a neuronal marker NeuN. Upper, GCL; under, Hilus. (C, C′) Morphological properties of Pax6$^+$ cells. (C) Many of Pax6$^+$ cells show radial glial shape and are often found in clusters in the SGZ. (C′) Pax6$^+$ cell has a GFAP$^+$ radial process. (D, D′, E, E′) Immuno-electron microscopy of Pax6$^+$ cells in the SGZ. P, Pax6$^+$ cells; G, granule cells; U, unknown cells. (D, E) Low magnification (× 1500) of Pax6$^+$ cells in the SGZ. (D′) High magnification (× 10 000) of Pax6$^+$ cell (magenta asterisk in D). Pax6$^+$ cell has irregular contours (magenta line, inset) and light cytoplasm containing a few ribosomes (r) and glial filaments (magenta arrows). Nuc, nucleus; mit, mitochondria. (E′) High magnification (× 5000) of Pax6$^+$ cell (yellow asterisk in E). Pax6$^+$ cells have smooth contours and dark scant cytoplasm negative for intermediate filaments.

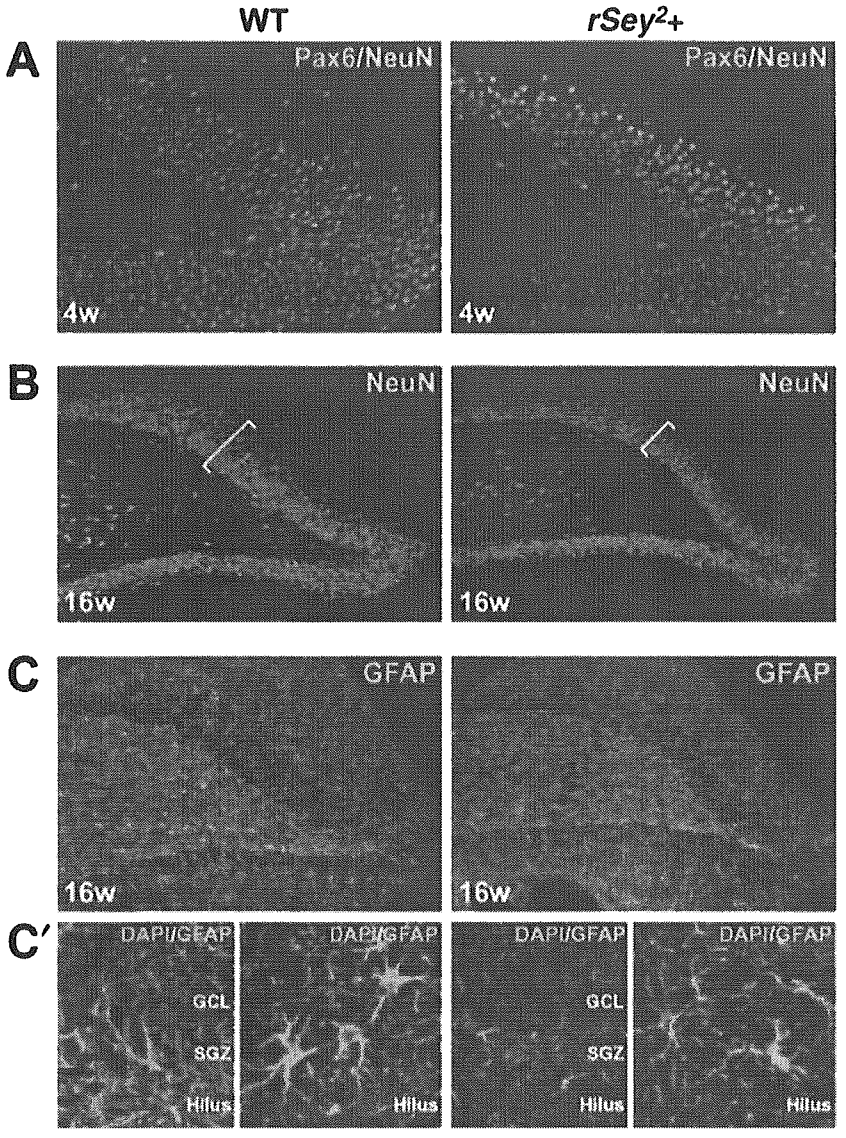


**Figure 2** Morphologic defects in DG of *rSey²*/+ rats. (A) In *rSey²*/+ rats at 4 weeks, Pax6-expressing cells are less in number and the expression level of Pax6 is remarkably decreased. (B) In *rSey²*/+ rats at 16 weeks, the thickness (bracket) of the granule cell layer (GCL) in the DG is thinner than that of WT. Granule cells are more packed in the GCL of *rSey²*/+ rats compared with the WT. (C) The number of GFAP$^+$ cells is less in the DG of *rSey²*/+ rats compared to WT. (C′) Radial glial fibers seem shorter and thinner in the DG of *rSey²*/+.

rat (*rSey²*). *rSey²* is a spontaneous mutant that has a nonsense mutation in the *Pax6* gene (Osumi *et al.* 1997), although truncated Pax6 protein is undetectable in the homozygote (our unpublished observation). Since homozygous *Pax6* mutant rats die at birth, heterozygotes (*rSey²*/+) were examined in this study. In the DG of *rSey²*/+ at 4 weeks, we found that the number of Pax6$^+$ cells reduced and that an expression level of Pax6 also decreased (Fig. 2A). We could not observe an apparent difference in the architecture of the DG in *rSey²*/+ rats at this stage.

At 16-week stage, we observed a prominent morphologic defect of the DG *rSey²*/+ rats: the GCL was much thinner and the density of granule cells was higher in the DG of *rSey²*/+ rats compared with the wild type (see brackets in Fig. 2B). We also noticed that the number of GFAP$^+$ cells was decreased and that the processes of GFAP$^+$ radial glial cells were thinner and underdeveloped in the DG of *rSey²*/+ rats (Fig. 2C,C′). This may explain in part why granule cells were more packed in the DG of *rSey²*/+ rats; there may be less spaces among granule cells because of thinner and underdeveloped radial glial processes. The previously mentioned character of Pax6-expressing cells in the DG of the wild type and the abnormalities in the DG of *rSey²*/+ rats raised a possibility that the total number of new neurons in postnatal hippocampus is decreased in the haplo-insufficient condition of the *Pax6* gene.

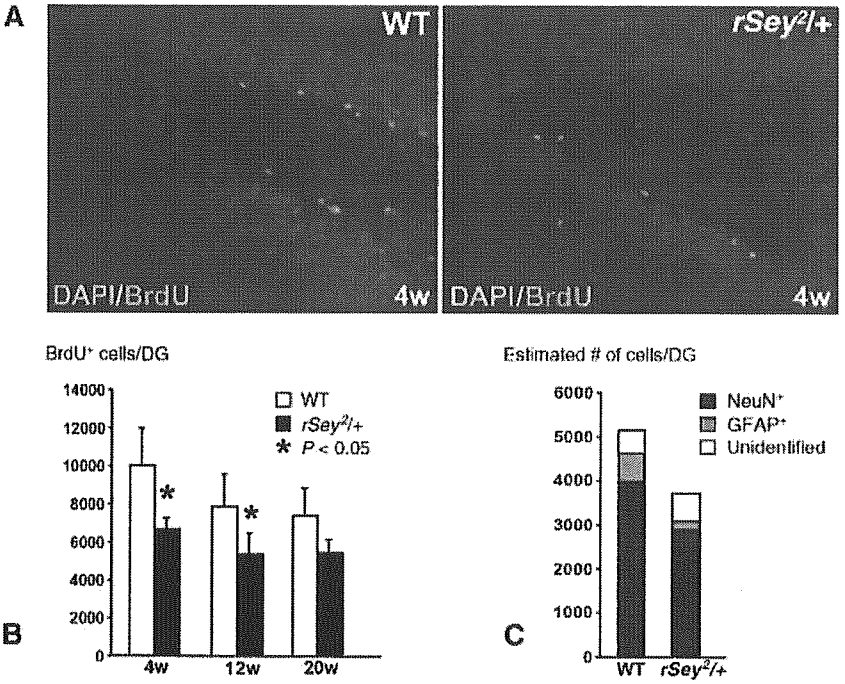


D

| | BudU⁺ cells | | | Developmental rate | |
|---|---|---|---|---|---|
| | 12 week $n = 6$ | 12 + 4week $n = 3$ | Survived | NeuN⁺ $n = 4$ | GFAP⁺ $n = 4$ |
| Wild type | 7853 ± 1663 | 5168 ± 120.6 | 65.8 ± 0.1% | 78.8 ± 8.2% | 12.6 ± 1.3% |
| *rSey²/+* | 5370 ± 1130 | 3712 ± 159.0 | 69.1 ± 0.1% | 77.7 ± 6.9% | 5.3 ± 1.0% |

Table. Survival rate and developmental fates of BrdU⁺ cells in the dentate gyrus

**Figure 3** Reduced cell proliferation and production of new neurons and astrocytes in the dentate gyrus of *rSey²/+* rats at postnatal stages. (A) The number of BrdU-positive cells (green) is decreased in the DG of *rSey²/+* rats after 3-day BrdU incorporation at 4 weeks. (B) The numbers of BrdU-positive cells within the DG are 33.3% ($P = 0.046$), 31.6% ($P = 0.021$), and 26.2% ($P = 0.051$) lower in the *rSey²/+* rats than in the wild-type at 4, 12, and 20 weeks, respectively. (C) Estimated numbers of cells double-positive for BrdU/NeuN (new neurons) and for BrdU/GFAP (new astroglia) based on the survival rate and the developmental fates shown in (D). Formation of new neurons and astroglia is markedly decreased in *rSey²/+* rats from 12 to 16 weeks. (D) Calculated survival rate and developmental fates of BrdU-positive cells in the DG 4 weeks after BrdU-injection at 12 weeks of age. The survival rate is not changed between WT and *rSey²/+*. In contrast, frequency of GFAP⁺ in total BrdU⁺ cells is less in *rSey²/+* at 4 weeks after BrdU injection, although that of frequency of NeuN⁺ in total BrdU⁺ cells is similar between WT and *rSey²/+* at 4 weeks after BrdU injection.

### Decreased cell proliferation in the DG of *rSey²/+* rats

To address the question whether postnatal neurogenesis is affected in the SGZ of *Pax6*-deficient rats, we first compared the total number of BrdU⁺ cells in the DG between the wild type and *rSey²/+* at 4, 12, and 20 weeks. Rats were intraperitoneally injected with BrdU three times a day for 3 days and sacrificed at 24 h after the last BrdU injection (Kempermann & Gage 1999). In the DG of the wild type, the total number of BrdU-labeled cells in the SGZ per hemisphere decreased as the stage proceeded (Fig. 3A,B). Interestingly, a significant decrease in the total number of BrdU-labeled cells was observed in *rSey²/+* at 4 weeks (33.3% decrease), 12 weeks (31.6%), and 20 weeks (26.2%) (Fig. 3B). These data clearly indicate that the number of proliferating progenitor cells is considerably reduced in the SGZ of *Pax6*-deficient rat.

Next, we examined the fate of newborn cells in the DG. The wild type and *rSey²/+* rats were injected with BrdU three times a day for 3 days at 12 weeks and examined 4 weeks later based on the previous protocol (Kempermann & Gage 1999). Although the proliferating rate was much decreased in the DG of *rSey²/+* (Fig. 3B), there were no differences in the survival rate of newborn cells between the wild type and *rSey²/+* (Fig. 3D). The percentage of NeuN⁺ cells in total BrdU⁺ cells (new neurons) was also unchanged in *rSey²/+* (Fig. 3D). Contrastingly, the percentage of GFAP⁺ cells in total BrdU⁺ cells decreased to less than half in *rSey²/+* (Fig. 3D). This is superficially considered to be a reduction of newborn astrocytes. However, it is now widely accepted that GFAP⁺ astrocytes can serve as neural stem cells in the hippocampus (Seri *et al.* 2001). Eventually, the estimated total numbers of newly generated neurons and astrocytes/progenitor cells were dramatically reduced in the DG of *Pax6*-deficient rat (Fig. 3C).

In a BrdU labeling study for a longer period (2 weeks), the ratio of BrdU⁺/Pax6⁺ cells in the wild type was increased up to fivefold (35%) comparing with the samples labeled for a short period (30 min) (7.7% at 4 week; 6.3% at 6 week). This may imply that a population of cells expressing Pax6 contain neural stem cells (or quiescent GFAP⁺ early progenitor cells) whose cell cycle is longer than that of GFAP⁺ early progenitor cells. We also found

that the number of Pax6$^+$/GFAP$^+$ double-positive cells in *rSey*$^2$/+ was 22% less than that in the WT at 4 week (WT, 482 578 ± 33 757 cells/mm$^3$; *rSey*$^2$/+, 374 981 ± 21 527 cells/mm$^3$; $n = 4$, $P < 0.01$). Furthermore, the number of BrdU$^+$/Pax6$^+$ double-positive cells was 27% decreased in *rSey*$^2$/+ rats (WT, 238 208 ± 27 545 cells/mm$^3$; *rSey*$^2$/+, 174 921 ± 13 478 cells/mm$^3$; $n = 4$, $P < 0.01$) in BrdU labeling study for a longer period (2 weeks). All these results consistently suggest that Pax6 is essential for proliferation of neural progenitor cells, thereby keeping the size of the progenitor pool.

### The number of GFAP$^+$ early progenitors decreased in the SGZ of *rSey*$^2$/+

To further elucidate the role of Pax6 in hippocampal neurognesis, we investigated at which step a transition of neurogenesis is impaired by detailed BrdU pulse/chase experiments combined with immunostaining with progenitor markers at 4 weeks. At the beginning, we re-examined the character of Pax6$^+$ cells in combination with BrdU labeling. Remarkably, more than 90% of total BrdU-incorporated cells in the SGZ expressed Pax6 at 30 min after BrdU injection (Fig. 4A,B). This result strongly suggests that Pax6 is vital for the cell proliferation in postnatal hippocampal neurogenesis. The fact that Pax6$^+$ cells are highly proliferative may also explain why they were often seen in clusters in the SGZ (Fig. 1A,C).

Then we investigated the cell-type transition of BrdU-incorporated cells in the SGZ of the wild-type and *Pax6*-deficient 4-week-old rats at 30 min, 24 h and 72 h after BrdU injection. In the wild type, the percentage of Pax6$^+$ cells in total BrdU$^+$ cells became markedly reduced from 30 min to 72 h, but 58% of BrdU$^+$ cells still expressed Pax6 at 72 h (Fig. 4B). The frequency of GFAP$^+$ in total BrdU$^+$ cells decreased between 30 min and 24 h after BrdU injection (Fig. 4C). Contrastingly, the ratio of PSA-NCAM$^+$ in total BrdU$^+$ cells increased between 30 min and 24 h after BrdU injection (Fig. 4D). These data are basically consistent with the results obtained in the mouse (Seri *et al.* 2001; Fukuda *et al.* 2003).

The same analyses were then performed on the DG of the *rSey*$^2$/+ rat. The percentage of Pax6$^+$ cells in total BrdU$^+$ cells slightly decreased but was statistically unchanged between the wild type and *rSey*$^2$/+ (Fig. 4B). In contrast, we found a significant decrease (38.4% decrease at 24 h; 49.6% decrease at 72 h, $P < 0.03$) in the frequency of GFAP$^+$ cells in total BrdU$^+$ cells (Fig. 4C) and an

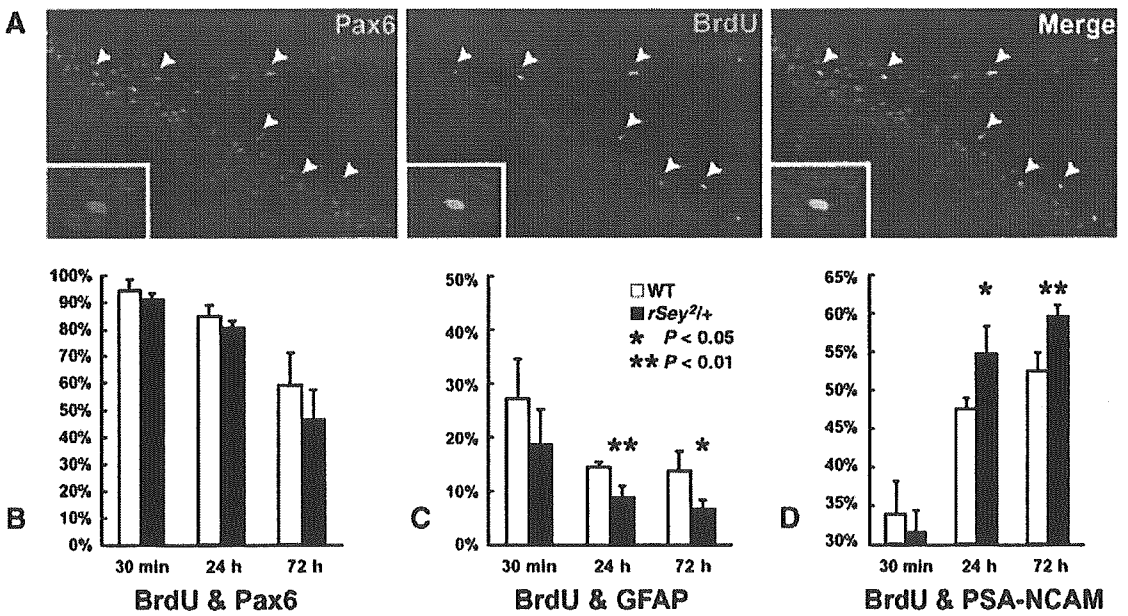


**Figure 4** BrdU pulse/chase labeling assay in the DG of the 4-week-old wild type (WT) and Pax6 deficient (*rSey*$^2$/+) rats. (A) Confocal micrographs of BrdU-labeled Pax6$^+$ cells 30 min after BrdU injection. Most of BrdU labeled cells co-express Pax6 (arrows). In *rSey*$^2$/+, the expression level of Pax6 protein is reduced and the number of Pax6$^+$ cells is less than in the wild type. (B–D) Percentage of BrdU-labeled cells in the SGZ at 30 min, 24 h, and 72 h after BrdU injection. (B) At 30 min, more than 90% of BrdU$^+$ cells co-express Pax6. From 30 min to 72 h, the number of Pax6$^+$ cells becomes markedly reduced in WT and *rSey*$^2$/+. (C) Frequency of GFAP$^+$ in total BrdU$^+$ cells is less in *rSey*$^2$/+ at 24 h and 72 h after BrdU injection. (D) Contrastingly, more PSA-NCAM$^+$ cells are observed in total BrdU$^+$ cells in *rSey*$^2$/+ at 24 h and 72 h after BrdU injection.

opposite increase (15.1% increase at 24 h; 13.5% increase at 72 h, $P < 0.03$) in PSA-NCAM$^+$ cells (Fig. 4D). These data clearly indicate that maintenance of GFAP$^+$ early progenitor cells is extremely impaired in the DG of *rSey*$^2$/+.

We performed BrdU pulse labeling study with a short survival period (5 days) to examine whether Pax6 accelerates the neuronal differentiation from dividing PSA-NCAM$^+$ late progenitor cells to NeuN expressing immature neurons. The ratio of NeuN$^+$/BrdU$^+$ cells in this study was unchanged between WT and *rSey*$^2$/+ (4w WT, 63.4%; 4w *rSey*$^2$/+, 66.6%; $n = 4$, $P = 0.36$). Therefore, Pax6 may not be involved in neuronal differentiation but in maintenance of the GFAP$^+$ early progenitor cells by regulating their proliferation.

We further examined how the character of neural progenitors in the DG was different between the wild type and *rSey*$^2$/+ at 4 weeks. As described previously, 31.5% of Pax6$^+$ cells co-expressed a marker for the late progenitor, PSA-NCAM (Figs 1B and 5C). Quite interestingly, Pax6$^+$/PSA-NCAM$^+$ cells dramatically increased up to 55.5% in *rSey*$^2$/+ rats (45/81 cells; 76% increase than that of wild type; Fig. 5B,C). Moreover, GFAP and PSA-NCAM double-positive cells were scarcely detected in the DG of WT rats, while such GFAP$^+$/PSA-NCAM$^+$ cells were quite often observed in the DG of *rSey*$^2$/+ rats (Fig. 5D). These results may imply that premature neuronal differentiation occurs in the DG of the *rSey*$^2$/+. As seen in 16-week rats (Fig. 2C,C′), the number of GFAP$^+$ cells was much less in the SGZ and hilus, and GFAP$^+$ cells have thin and underdeveloped processes in *rSey*$^2$/+ rats (Fig. 5A,E). Quantitatively, the level of GFAP expression was 16% less in the mutant hippocampus as judged from real-time polymerase chain reaction (PCR) (data not shown). These results suggest that hippocampal neurogenesis is quite abnormal in *Pax6*-deficient rat. All the findings consistently suggest a pivotal role of Pax6 in maintenance of the GFAP$^+$ early progenitor cells in the postnatal hippocampus.

### Wnt signaling is impaired in the DG of *rSey*$^2$/+

What kinds of molecules then regulate cell proliferation under the control of Pax6 transcription factor? Among various candidate factors, we focused on Wnt signaling molecules because their expressions are reported in the postnatal DG (Shimogori *et al.* 2004) and also because we ourselves have shown down-regulation of a Wnt ligand expression in *rSey*$^2$/*rSey*$^2$ rat embryos (Osumi *et al.* 1997; Takahashi *et al.* 2002).

We first searched expression patterns of various Wnt signaling molecules by performing *in situ* hybridization of genes encoding Wnt ligands, Frizzled receptors, and a downstream molecule Dvl1. Among them, *Wnt7a*, *Wnt7b*, *Fz3*, and *Dvl1* showed interesting expression patterns in the DG for 3–4 weeks (Fig. 6). *Wnt7a*, a Wnt ligand, was preferentially expressed in the hilus and along the SGZ of the blades of the DG. Another Wnt ligand, *Wnt7b*, was detected in the SGZ and the GCL, but *Wnt7b*-expressing cells did not morphologically seem to be granule cells in the GCL. Weak expression of *Wnt3a* was also detected in the SGZ at 2 weeks, but almost diminished by 4 weeks in the rat (data not shown). These expression patterns of Wnt ligands hint us to imagine that they are expressed in the progenitors themselves or other cells that may constitute a niche for keeping the undifferentiated state of the progenitor cells. In the DG of *rSey*$^2$/+, the number of *Wnt7a*-expressing cells significantly decreased (687 cells in the wild type; 576 cells in *rSey*$^2$/+; 16% decrease), and the number of *Wnt7b*-expressing cells also decreased (607 in the wild type; 544 in *rSey*$^2$/+; 11% decrease). We could not observe any difference in expression of *Wnt3a* in the DG of *rSey*$^2$/+. Expression of a Wnt receptor *Fz3* was detected mainly in the GCL, and unchanged in the DG of *rSey*$^2$/+. Contrastingly, the expression level of *Dvl1* was increased in the DG of *rSey*$^2$/+ (Fig. 6). Taken altogether, Wnt signaling is impaired in the DG under the Pax6 deficient condition, which may result in reduced proliferation of GFAP$^+$ early progenitor cells in *rSey*$^2$/+.

## Discussion

### Pax6 expressed in GFAP$^+$ early progenitor cells in hippocampal neurogenesis

Previous papers suggest that adult hippocampal neurogenesis originates from precursor cells in the DG and results in new granule neurons through multiple steps from the GFAP$^+$ early progenitor cells to the PSA-NCAM$^+$ late progenitor cells (Seri *et al.* 2001; Fukuda *et al.* 2003; Kempermann *et al.* 2004). In the present study, we revealed that Pax6$^+$ cells frequently co-expressed GFAP and Musashi1, sometimes expressed nestin and PSA-NCAM, but scarcely co-expressed NeuN in the SGZ of the postnatal DG (Fig. 1B). That is, Pax6 is considered to be expressed mostly in the GFAP$^+$ early progenitor cells.

The ratio of nestin-positive cells among BrdU$^+$ was less than that in a previous study using nestin-EGFP reporter mice (Filippov *et al.* 2003; Fukuda *et al.* 2003). This may be due to difference in sensitivity of anti-nestin antibody and duration of nestin-promoter-driven EGFP. More importantly, a large number of Pax6$^+$/GFAP$^+$ cells had early progenitor-like morphology with a long radial

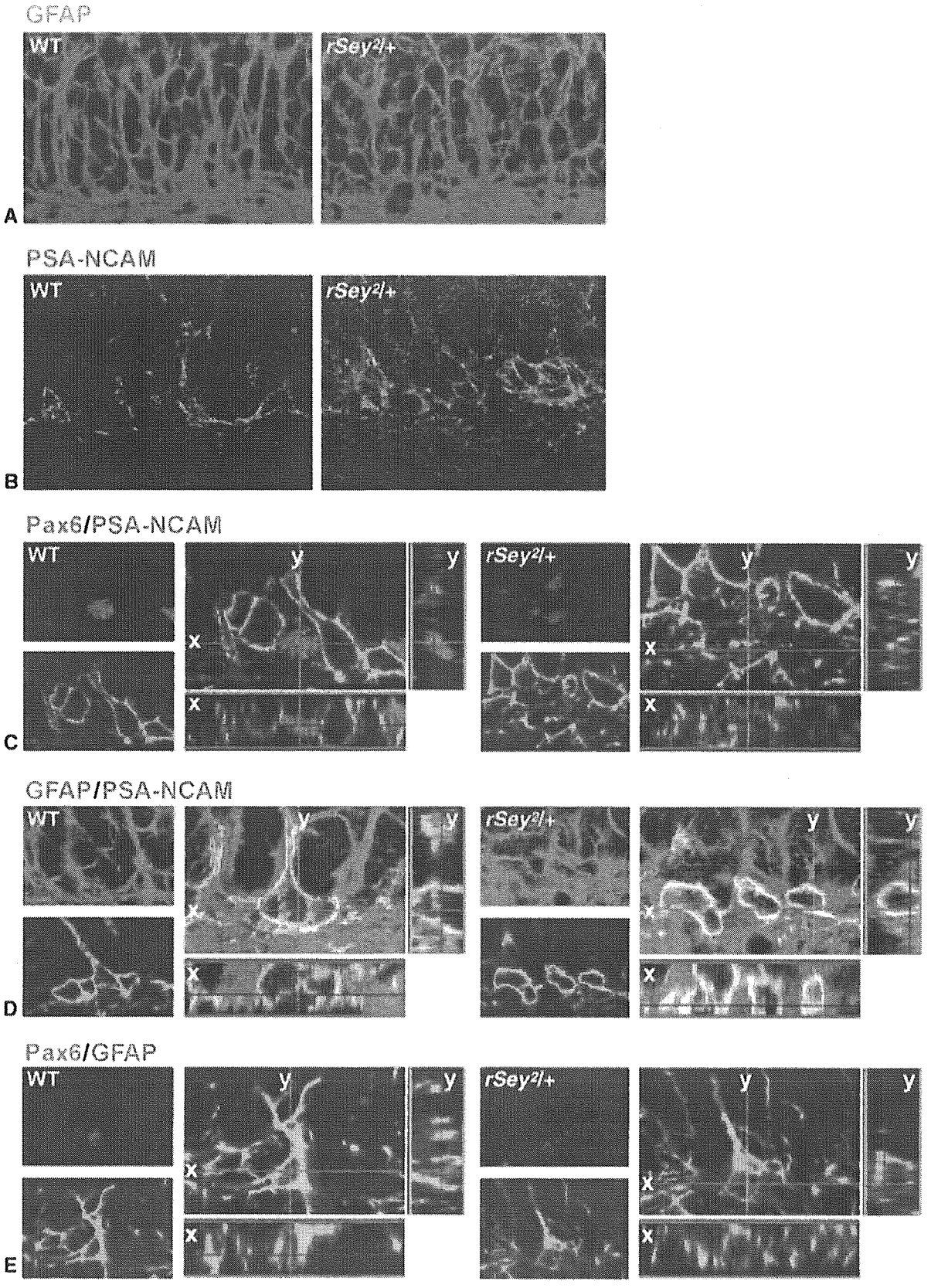

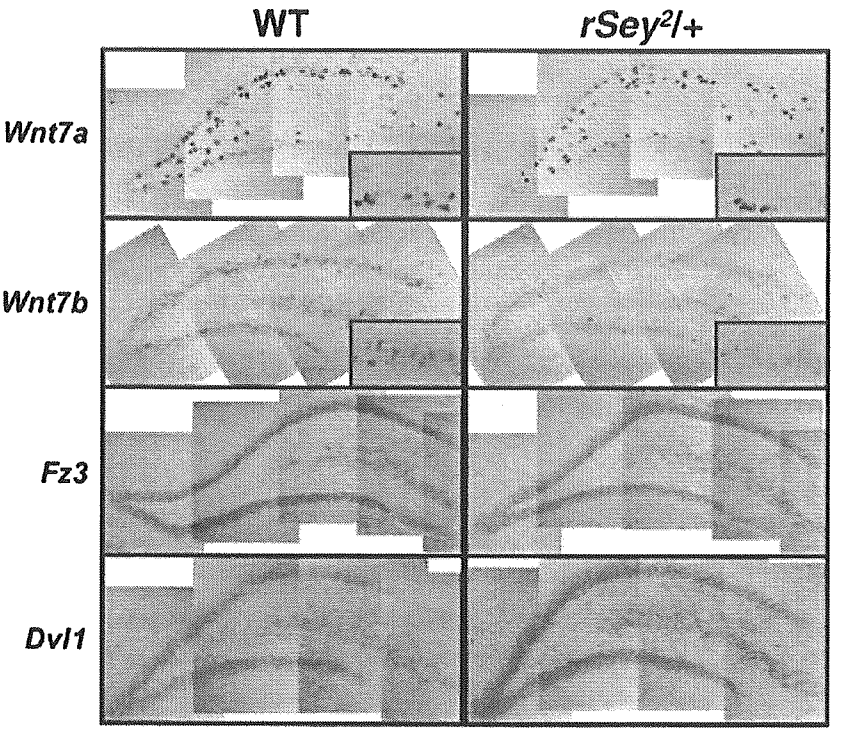


**Figure 6** Altered expressions of Wnt-signaling molecules in the DG of *rSey²/+*. In the hippocampus of wild-type, *Wnt7a* is expressed in the SGZ and hilus, while *Wnt7b*, *Fz3*, and *Dvl1* are expressed in the GL and SGZ. In the hippocampus of *rSey²/+*, the number of *Wnt7a*- and *Wnt7b*-expressing cells was decreased, and the expression level of *Wnt7b* was down-regulated. Contrastingly, the expression level of *Dvl1* was increased in the DG of *rSey²/+*. No difference between the wild-type and *rSey²/+* was observed in the expression level of *Fz3*.

process (Fig. 1C′), and Pax6$^+$/nestin$^+$ mostly showed a GFAP$^+$ early progenitor shape (Fig. 1B) and sometimes a PSA-NCAM$^+$ late progenitor cell shape. Pax6$^+$ cells sometimes co-expressed PSA-NCAM, but such Pax6$^+$/PSA-NCAM$^+$ cells always exhibited the late progenitor cell-like morphology. From immuno-electron microscopy, we found that the majority of Pax6$^+$ cells showed features corresponding to type B cells, and that a small number of Pax6$^+$ cells had characters corresponding to type D cells, while Pax6$^+$ cells never showed phenotypes of granule cells (Fig. 1D,D′, E,E′). Therefore, it is concluded that more than half of Pax6$^+$ cells have the character of the GFAP$^+$ early progenitor cells in the SGZ of the hippocampus (Fig. 7).

At present there are no good markers that properly distinguish quiescent neural stem cells from the progenitor cells in the hippocampal neurogenesis. However, we found that the ratio of BrdU$^+$ cells in Pax6$^+$ cells increased fivefold in a 2-week BrdU labeling compared to that in a 30-min labeling. It is thus likely that a population of Pax6-expressing cells may include the quiescent neural stem/progenitor cells in the hippocampus.

**Figure 5** Abnormal PSA-NCAM$^+$ cells and GFAP$^+$ cells in *rSey²/+* rats at 4 weeks. (A) In *rSey²/+* rats, there are fewer GFAP$^+$ cells whose processes are thin and underdeveloped. (B) PSA-NCAM$^+$ cells are increased in number and abnormally colonized at the SGZ in *rSey²/+* rats. (C) In the wild-type (WT) rat, PSA-NCAM$^+$ cells scarcely co-express Pax6. Contrastingly, many Pax6$^+$ cells co-express PSA-NCAM in *rSey²/+* rat. In *rSey²/+* rat, Pax6 expression is down-regulated comparing with WT. (D) In the WT rat, PSA-NCAM$^+$ cells scarcely co-express GFAP. Contrastingly, many PSA-NCAM$^+$ cells co-express GFAP in *rSey²/+* rat. (E) In the WT and *rSey²/+* rats, a GFAP$^+$ radial glial cell co-expresses Pax6. In the *rSey²/+* rat, a process of the GFAP+ radial glial cell is thin and undeveloped, and the expression of Pax6 is reduced.

### The role of Pax6 in postnatal hippocampus

As discussed above, Pax6$^+$ cells have the character of neural stem cells and GFAP$^+$ early progenitor cells in the DG of postnatal hippocampus. It is thus expected that Pax6 is involved in cell proliferation and/or cell differentiation in hippocampal neurogenesis.

There are some papers where Pax6 is involved in cell proliferation in developing cortex (Warren *et al.* 1999). We found from BrdU labeling analyses that cell proliferation was dramatically reduced in the *Pax6*-deficient DG (Fig. 2A). In addition, more than 90% of total BrdU$^+$ cells were Pax6-positive at 30 min after BrdU injection in the SGZ of adult hippocampus (Fig. 4A,B). These data

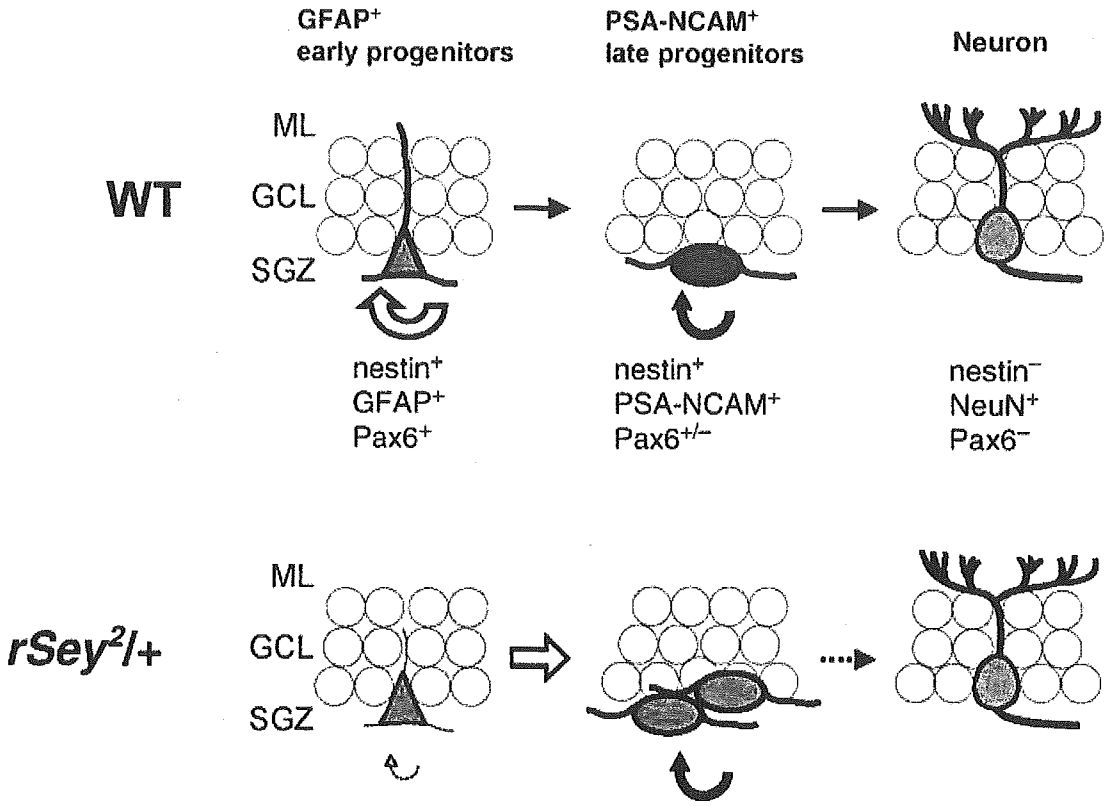


**Figure 7** The role of Pax6 in adult hippocampal neurognesis. Distinct progenitor cells are identified on the basis of morphology, proliferative activity, and marker expressions. In the wild type (WT), GFAP$^+$ early progenitors have a radial glial appearance with the cell body in the subgranular zone (SGZ) of the dentate gyrus, and also express nestin and Pax6. PSA-NCAM$^+$ late progenitors have plump short processes that are oriented tangentially, and they are nestin$^{+/-}$, GFAP-, PSA-NAM$^+$ and Pax6$^{+/-}$. Mature neurons in the granule cell layer (GCL) retain a vertical morphology with a rounded or slightly triangular nucleus and clearly visible apical dendrites, and they are nestin$^-$, Pax6$^-$, and NeuN$^+$. In *Pax6* deficient condition (*rSey*$^2$/+), GFAP$^+$ early progenitors have a thinner and undeveloped radial process and are fewer in number than in the WT. There is a more rapid shift from the GFAP$^+$ early progenitor cells to the PSA-NCAM$^+$ late progenitor cells in *rSey*$^2$/+ (big arrow). These PSA-NCAM$^+$ late progenitors show abnormal morphology, ectopic location, and altered molecular character (i.e. increased PSA-NCAM$^+$/Pax6$^+$ and PSA-NCAM$^+$/GFAP$^+$ double positive cells). That is, production of the early progenitor cells is impaired in *Pax6* deficient condition, thereby generating fewer neurons (dotted arrow).

strongly suggest that Pax6 is vital for the cell proliferation in the hippocampal neurogenesis. Then, for which steps of the neurogenesis is Pax6 required in cell proliferation?

Previous papers report that both GFAP$^+$ early progenitor cells and PSA-NCAM$^+$ late progenitor cells are transit amplifying cells. Rapid transition from GFAP$^+$ early progenitors/type B cells to PSA-NCAM$^+$ late progenitors/type D cells occurs between 2 and 24 h after the BrdU single injection (Seri *et al.* 2001; Fukuda *et al.* 2003). In the similar experiment, we found dramatic decrease in the number of GFAP$^+$/BrdU$^+$ cells and an inverse increase in the number of PSA-NCAM$^+$/BrdU$^+$ cells in the SGZ of the *rSey*$^2$/+ (Fig. 4C,D). Moreover, the morphology of GFAP$^+$ cells was altered in *rSey*$^2$/+ (Figs 2C′, 5A, 5E). Our findings suggest that the maintenance of the GFAP$^+$ early progenitor cells is perturbed in the DG of the *rSey*$^2$/+, presumably resulting in a more rapid shift from the GFAP$^+$ early progenitors to the PSA-NCAM$^+$ late progenitors (Fig. 7).

There are some reports that Pax6 promotes neuronal differentiation in the developing cortex and adult SVZ (Heins *et al.* 2002; Hack *et al.* 2004, 2005). To test the possibility that Pax6 is involved in neuronal differentiation in the postnatal hippocampus, we examined the ratio of NeuN$^+$/total BrdU$^+$ cells at 5 days time point after the BrdU injection in *rSey*$^2$/+. The ratio of NeuN$^+$/BrdU$^+$ cells in *rSey*$^2$/+ was not different from that in the WT, even though there is a more rapid shift from the

GFAP$^+$ early progenitor cells to the PSA-NCAM$^+$ late progenitor cells in *rSey²*/+. Therefore, such abnormally differentiated PSA-NCAM$^+$ late progenitor cells did not effectively contribute to produce neurons. In fact, these PSA-NCAM$^+$ late progenitor cells exhibited abnormal characters; they often retained GFAP expression, which is hardly observed in the WT, and did not line up at the SGZ but colonized in disorganized positions (Fig. 5B,D). Since we observed increased cell death in *rSey²*/+ (M.M. and N.O., unpublished observation), such functionally abnormal PSA-NCAM$^+$ late progenitor cells may eventually die off in the SGZ of the *rSey²*/+. Taken altogether, Pax6 functions in cell proliferation rather than differentiation in the DG.

We found a marked decrease of the percentage of GFAP$^+$ in BrdU$^+$ cells in *rSey²*/+ compared with the wild type, while no significant difference was detected in the percentage of NeuN$^+$ in all BrdU$^+$ cells at 4 weeks after the BrdU injection (Fig. 3C,D). However, since the total number of BrdU$^+$ cells dramatically decreased in *rSey²*/+, newly generated granule cells were markedly reduced in *rSey²*/+ rat. Eventually, at 16 weeks, the GCL became thinner in the DG of *rSey²*/+ rats than that of the wild type (Fig. 2B). Therefore, it is suggested that Pax6 primarily functions to maintain the progenitor pool in the hippocampus; if the size of the progenitor pool is reduced by Pax6 haplo-insufficiency, the subsequent production of neurons is severely impaired.

The number of Pax6$^+$/GFAP$^+$ cells, BrdU$^+$ cells (BrdU labeling three times a day for 3 days) and BrdU$^+$/Pax6$^+$ cells (BrdU labeling two times a day for 2 weeks) were already more reduced in *rSey²*/+ rats than in WT rats at the earliest time point we observed (4 weeks). Therefore, it is possible that Pax6 is necessary for the production of GFAP$^+$ early progenitor cells during the initial formation of the hippcampus. This is quite reasonable because we observed that extremely less GFAP$^+$ cells (including not only those mature astrocytes but also neural stem/progenitor cells) were produced in the DG of *rSey²*/+ rats (Fig. 3C,D). Taken all together, it is concluded that Pax6 is necessary for keeping a good balance between cell proliferation and differentiation in the hippocampal neurogenesis (Fig. 7).

### Pax6–Wnt pathway in hippocampal neurogenesis

Because Pax6 is a transcription factor, its influence on the production of GFAP$^+$ early progenitor cells is naturally brought by transcriptional regulation of other genes. Although several secreted molecules such as EGF, FGF2, BDNF, and Shh have been known to regulate adult neurogenesis (Craig *et al.* 1996; Kuhn *et al.* 1997; Tropepe *et al.* 1997; Zigova *et al.* 1998; Machold *et al.* 2003), we could not find any difference in expression of these molecules in the DG of *rSey²*/+ rats (not shown). However, we have found dramatically different expression patterns of genes involved in Wnt signaling pathway.

Wnt genes encode secreted proteins that regulate fate decisions of various cells depending on the context. The functions of Wnt signaling are studied intensively in many aspects of embryogenesis such as anterior–posterior axis formation, cell type specification, cell proliferation, and axonal growth (Patapoutian & Reichardt 2000; Wang & Wynshaw-Boris 2004; Zou 2004). Although Wnt signaling in the postnatal brain has been comparatively little investigated, a recent report describes remarkably patterned gene expressions of Wnt signaling components in the postnatal mouse brain including the hippocampus (Shimogori *et al.* 2004). In addition, Wnt signaling has already been reported to be altered in embryonic brains of *Pax6* mutant mice and rats (Grindley *et al.* 1997; Osumi *et al.* 1997; Warren & Price 1997; Kim *et al.* 2001; Takahashi *et al.* 2002). We found specific expression of *Wnt7a* and *Wnt7b* in the wild-type SGZ, and marked reduction of *Wnt7a* and *Wnt7b* expressions in the DG of the *rSey²*/+. Conversely, *Dv1* was up-regulated in the DG of the *rSey²*/+ (Fig. 6). Therefore, Wnt signaling is altered in the *Pax6*-deficient DG.

During cortical development, Wnt signaling has multiple and stage-specific roles. In early embryonic stages, Wnt7a, 7b, and stabilized β-catenin promote self-renewal of neural precursor cells and suppress neural differentiation (Chenn & Walsh 2002; Viti *et al.* 2003). On the other hand, it is reported that the Wnt/β-catenin pathway directs neuronal differentiation of the cortical precursor cells at later developmental stages (Hirabayashi *et al.* 2004). Curiously, in adult hippocampus, lithium facilitates proliferation and differentiation of progenitor cells to a specific neural cell type by perturbing functions of GSK3β, a pivotal player not only in the PI3 kinase pathway but also in Wnt/β-catenin pathway (Chen *et al.* 2000; Kim *et al.* 2004). In the present study, we found that specific expressions of Wnt ligands in the SGZ and that Wnt signaling is altered in the DG of *Pax6*-deficient rat (Fig. 6) suggest an intriguing possibility that impaired Wnt signaling may perturb the production of GFAP$^+$ early progenitor cells in postnatal hippocampus. Expression patterns of *Wnt7a* and *7b* may also support the idea that cells expressing Wnt ligands constitute an environment as a stem cell niche to maintain neural progenitor cells. It would be important to elucidate how Pax6-Wnt signaling coordinately regulates proliferation of neural stem cells/GFAP$^+$ early progenitor cells in the SGZ.

## Experimental procedures

### Animals

Large colonies of heterozygous *Pax6* mutant rats (*rSey²*/+) and wild-type Sprague–Dawley (SD) rats (littermates of *rSey²*/+ rats) were maintained at Tohoku University School of Medicine and National Institute of Neuroscience. The genotype of *rSey²*/+ rats was distinguishable based on the presence of eye defects. All animal experiments were carried out in accordance with the National Institute of Health guidelines for the care and use of laboratory animals and were approved by the Committee for Animal Experiments in the aforementioned organizations.

### Tissue preparation

Rats were deeply anesthetized with diethyl ether or pentobarbital sodium before sacrifice. Brains were perfused transcardially with 4% paraformaldehyde (PFA) in 0.01 M PBS (sodium phosphate buffer, pH 7.4) or 4% PFA and 0.5% picric acid in 0.01 M PBS, or 2% PFA and 2.5% glutaraldehyde in 0.01 M PBS, for immunohistochemistry, immuno-electron microscopic analysis, and conventional electron microscopic analysis, respectively. The brains were incubated in the same fixative for 2 h at 4 °C and cut into 70 μm coronal sections with a vibratome (Leica) or cut by a cryostat (Leica) into 14 μm sagittal sections.

### Immunohistochemistry

Procedures were basically according to the previous reports (Osumi *et al.* 1997; Fukuda *et al.* 2003). Detailed information will be provided on request. Antibodies against Musashi, nestin, and PSA-NCAM are kind gifts from Drs Hideyuki Okano, Masaharu Ogawa, and Tatsunori Seki (Miyata & Ogawa 1994; Seki & Arai 1999; Kaneko *et al.* 2000). Fluorescent signals were detected using a confocal laser-scanning microscope (Leica) or a fluorescent microscope (Axioplan-2, Zeiss).

### BrdU labeling analyses

Four-week-old rats received single intraperitoneal injections of 5-bromo-2-deoxyuridine (BrdU) (Sigma, St. Louis, MO) at 50 μg/kg body weight (10 mg/mL stock, dissolved in 0.9% saline), and were sacrificed at 30 min, 24 h, and 72 h after the injection (Seri *et al.* 2001; Kempermann *et al.* 2004). For cell fate analyses, 4-, 12- or 20-week-old rats received similar injections of BrdU three times a day for 3 days, and were sacrificed at day 1 or 4 weeks later (Kempermann & Gage 1999). For quiescent stem cell analysis, 4-week-old rats received injections of BrdU twice a day for 14 days, and were sacrificed 1 day later (Magavi *et al.* 2000). Seventy micrometers free-floating sections were cut and incubated in 2 N HCl for 1 h at room temperature, and washed in 0.01 M PBS (Saegusa *et al.* 2004). Otherwise, 14 μm frozen sections were boiled in 0.01 M citric acid and incubated in 2 N HCl for 10 min at 37 °C, and washed in 0.01 M PBS.

### Quantification

For BrdU pulse/chase examination, percentages of $Pax6^+$, $GFAP^+$, or PSA-$NCAM^+$ in total $BrdU^+$ cells were calculated in three sections per hemisphere. For quantification analysis, sampling of BrdU-positive cells was performed throughout the DG in its rostrocaudal extension. Every sixth section (14 μm) was used for counting, and the total number was obtained by multiplying the value by 6 (Kempermann & Gage 1999). For the fate analysis, $BrdU^+$/$NeuN^+$ in total $BrdU^+$ cells and $BrdU^+$/$GFAP^+$ in total $BrdU^+$ cells were counted in three adjacent sections in the same rostrocaudal regions of a DG (Kempermann & Gage 1999). For the quantification of the number of $GFAP^+$/$Pax6^+$ double-positive cells and $Pax6^+$/$BrdU^+$ double-positive cells, we counted these cells within the limited range in six adjacent sections and calculated the density. The number of these cells was counted in the blind manner.

### Electron microscopy

Procedures were basically according to the previous reports (Yuasa *et al.* 1996; Saegusa *et al.* 2004). Detailed information will be provided on request. These ultrathin sections were stained with lead citrate and uranyl acetate, and observed under a Hitachi H-7000 electron microscope.

### *In situ* hybridization

Procedures were basically according to the previous reports (Osumi *et al.* 1997; Takahashi *et al.* 2002). *Wnt7a*- and *Wnt7b*-expressing cells were counted on three adjacent sections in the same rostrocaudal region of a DG.

### Statistical analysis

Statistical analyses were performed with Microsoft Excel (Office 98), and ANOVA or two-sided *t*-test was applied when appropriate.

## Acknowledgements

We thank Drs Kazunobu Sawamoto, Tatsunori Seki, Toshiya Manabe, and Fiona Doetsch for the kind exchange of unpublished results and discussions and Drs Hideyuki Okano, Masaharu Ogawa, and Tatsunori Seki for valuable antibodies. We are also grateful to Drs Yoshiro Toyama and Yoshimichi Kozuka for the advice and support on the electron microscopic observations. We also thank Ms. Michi Otonari and Hisako Yusa for maintenance of the *rSey²* rat colony, and Ms. Yumi Watanabe for technical assistance. This work was supported by grant-in-aid #16047202 for Scientific Research on Priority Areas from the Ministry of Education, Culture, Sports, Science and Technology of Japan, and Japanese Science and Technology Corporation given to N.O., T.N., and K.I.

## References

Altman, J. & Das, G.D. (1965) Autoradiographic and histological evidence of postnatal hippocampal neurogenesis in rats. *J. Comp. Neurol.* **124**, 319–335.

Alvarez-Buylla, A., Seri, B. & Doetsch, F. (2002) Identification of neural stem cells in the adult vertebrate brain. *Brain Res. Bull.* **57**, 751–758.

Chen, G., Rajkowska, G., Du, F., Seraji-Bozorgzad, N. & Manji, H.K. (2000) Enhancement of hippocampal neurogenesis by lithium. *J. Neurochem.* **75**, 1729–1734.

Chenn, A. & Walsh, C.A. (2002) Regulation of cerebral cortical size by control of cell cycle exit in neural precursors. *Science* **297**, 365–369.

Craig, C.G., Tropepe, V., Morshead, C.M., *et al.* (1996) *In vivo* growth factor expansion of endogenous subependymal neural precursor cell population in the adult mouse brain. *J. Neurosci.* **16**, 2649–2658.

Doetsch, F., Caille, I., Lim, D.A., Garcia-Verdugo, J.M. & Alvarez-Buylla, A. (1999) Subventricular zone astrocytes are neural stem cells in the adult mammalian brain. *Cell* **97**, 703–716.

Doetsch, F., Garcia-Verdugo, J.M. & Alvarez-Buylla, A. (1997) Cellular composition and three-dimensional organization of the subventricular germinal zone in the adult mammalian brain. *J. Neurosci.* **17**, 5046–5061.

Estivill-Torrus, G., Pearson, H., van Heyningen, V., Price, D.J. & Rashbass, P. (2002) Pax6 is required to regulate the cell cycle and the rate of progression from symmetrical to asymmetrical division in mammalian cortical progenitors. *Development* **129**, 455–466.

Filippov, V., Kronenberg, G., Pivneva, T., *et al.* (2003) Subpopulation of nestin-expressing progenitor cells in the adult murine hippocampus shows electrophysiological and morphological characteristics of astrocytes. *Mol. Cell. Neurosci.* **23**, 373–382.

Forster, E., Tielsch, A., Saum, B., *et al.* (2002) Reelin, Disabled 1, and beta 1 integrins are required for the formation of the radial glial scaffold in the hippocampus. *Proc. Natl. Acad. Sci. USA* **99**, 13178–13183.

Fujita, S. (2003) The discovery of the matrix cell, the identification of the multipotent neural stem cell and the development of the central nervous system. *Cell Struct. Funct.* **28**, 205–228.

Fukuda, S., Kato, F., Tozuka, Y., *et al.* (2003) Two distinct subpopulations of nestin-positive cells in adult mouse dentate gyrus. *J. Neurosci.* **23**, 9357–9366.

Fukuda, T., Kawano, H., Osumi, N., Eto, K. & Kawamura, K. (2000) Histogenesis of the cerebral cortex in rat fetuses with a mutation in the Pax-6 gene. *Brain Res. Dev. Brain Res.* **120**, 65–75.

Gage, F.H. (2000) Mammalian neural stem cells. *Science* **287**, 1433–1438.

Gotz, M. (2003) Glial cells generate neurons—master control within CNS regions: developmental perspectives on neural stem cells. *Neuroscientist* **9**, 379–397.

Gotz, M., Stoykova, A. & Gruss, P. (1998) Pax6 controls radial glia differentiation in the cerebral cortex. *Neuron* **21**, 1031–1044.

Grindley, J.C., Hargett, L.K., Hill, R.E., Ross, A. & Hogan, B.L. (1997) Disruption of PAX6 function in mice homozygous for the Pax6Sey-1Neu mutation produces abnormalities in the early development and regionalization of the diencephalon. *Mech. Dev.* **64**, 111–126.

Hack, M.A., Saghatelyan, A., de Chevigny, A., *et al.* (2005) Neuronal fate determinants of adult olfactory bulb neurogenesis. *Nature Neurosci.*

Hack, M.A., Sugimori, M., Lundberg, C., Nakafuku, M. & Gotz, M. (2004) Regionalization and fate specification in neurospheres: the role of Olig2 and Pax6. *Mol. Cell. Neurosci.* **25**, 664–678.

Heins, N., Malatesta, P., Cecconi, F., *et al.* (2002) Glial cells generate neurons: the role of the transcription factor Pax6. *Nature Neurosci.* **5**, 308–315.

Hirabayashi, Y., Itoh, Y., Tabata, H., *et al.* (2004) The Wnt/beta-catenin pathway directs neuronal differentiation of cortical neural precursor cells. *Development* **131**, 2791–2801.

Kaneko, Y., Sakakibara, S., Imai, T., *et al.* (2000) Musashi1: an evolutionally conserved marker for CNS progenitor cells including neural stem cells. *Dev. Neurosci.* **22**, 139–153.

Kempermann, G. & Gage, F.H. (1999) Experience-dependent regulation of adult hippocampal neurogenesis: effects of long-term stimulation and stimulus withdrawal. *Hippocampus* **9**, 321–332.

Kempermann, G., Gast, D., Kronenberg, G., Yamaguchi, M. & Gage, F.H. (2003) Early determination and long-term persistence of adult-generated new neurons in the hippocampus of mice. *Development* **130**, 391–399.

Kempermann, G., Jessberger, S., Steiner, B. & Kronenberg, G. (2004) Milestones of neuronal development in the adult hippocampus. *Trends Neurosci.* **27**, 447–452.

Kim, A.S., Anderson, S.A., Rubenstein, J.L., Lowenstein, D.H. & Pleasure, S.J. (2001) Pax-6 regulates expression of SFRP-2 and Wnt-7b in the developing CNS. *J. Neurosci.* **21**, RC132.

Kim, J.S., Chang, M.Y., Yu, I.T., *et al.* (2004) Lithium selectively increases neuronal differentiation of hippocampal neural progenitor cells both in vitro and in vivo. *J. Neurochem.* **89**, 324–336.

Kuhn, H.G., Dickinson-Anson, H. & Gage, F.H. (1996) Neurogenesis in the dentate gyrus of the adult rat: age-related decrease of neuronal progenitor proliferation. *J. Neurosci.* **16**, 2027–2033.

Kuhn, H.G., Winkler, J., Kempermann, G., Thal, L.J. & Gage, F.H. (1997) Epidermal growth factor and fibroblast growth factor-2 have different effects on neural progenitors in the adult rat brain. *J. Neurosci.* **17**, 5820–5829.

Machold, R., Hayashi, S., Rutlin, M., *et al.* (2003) Sonic hedgehog is required for progenitor cell maintenance in telencephalic stem cell niches. *Neuron* **39**, 937–950.

Magavi, S.S., Leavitt, B.R. & Macklis, J.D. (2000) Induction of neurogenesis in the neocortex of adult mice. *Nature* **405**, 951–955.

Miyata, T. & Ogawa, M. (1994) Developmental potentials of early telencephalic neuroepithelial cells: a study with microexplant culture. *Dev. Growth Differ.* **36**, 319–331.

Nakatomi, H., Kuriu, T., Okabe, S., *et al.* (2002) Regeneration of hippocampal pyramidal neurons after ischemic brain injury by recruitment of endogenous neural progenitors. *Cell* **110**, 429–441.

Osumi, N. (2001) The role of Pax6 in brain patterning. *Tohoku J. Exp. Med.* **193**, 163–174.

Osumi, N., Hirota, A., Ohuchi, H., *et al.* (1997) Pax-6 is involved in the specification of hindbrain motor neuron subtype. *Development* **124**, 2961–2972.

Patapoutian, A. & Reichardt, L.F. (2000) Roles of Wnt proteins in neural development and maintenance. *Curr. Opin. Neurociol.* **10**, 392–399.

Saegusa, T., Mine, S., Iwasa, H., *et al.* (2004) Involvement of highly polysialylated neural cell adhesion molecule (PSA-NCAM)-positive granule cells in the amygdaloid-kindling-induced sprouting of a hippocampal mossy fiber trajectory. *Neurosci. Res.* **48**, 185–194.

Seki, T. & Arai, Y. (1993) Highly polysialylated neural cell adhesion molecule (NCAM-H) is expressed by newly generated granule cells in the dentate gyrus of the adult rat. *J. Neurosci.* **13**, 2351–2358.

Seki, T. & Arai, Y. (1999) Different polysialic acid-neural cell adhesion molecule expression patterns in distinct types of mossy fiber boutons in the adult hippocampus. *J. Comp. Neurol.* **19**, 115–125.

Seri, B., Garcia-Verdugo, J.M., McEwen, B.S. & Alvarez-Buylla, A. (2001) Astrocytes give rise to new neurons in the adult mammalian hippocampus. *J. Neurosci.* **21**, 7153–7160.

Shimogori, T., VanSant, J., Paik, E. & Grove, E.A. (2004) Members of the Wnt, Fz, and Frp gene families expressed in postnatal mouse cerebral cortex. *J. Comp. Neurol.* **473**, 496–510.

Simpson, T.I. & Price, D.J. (2002) Pax6; a pleiotropic player in development. *Bioessays* **24**, 1041–1051.

Stoykova, A., Gotz, M., Gruss, P. & Price, J. (1997) Pax6-dependent regulation of adhesive patterning, R-cadherin expression and boundary formation in developing forebrain. *Development* **124**, 3765–3777.

Stoykova, A. & Gruss, P. (1994) Roles of Pax-genes in developing and adult brain as suggested by expression patterns. *J. Neurosci.* **14**, 1395–1412.

Takahashi, M., Sato, K., Nomura, T. & Osumi, N. (2002) Manipulating gene expressions by electroporation in the developing brain of mammalian embryos. *Differentiation* **70**, 155–162.

Tramontin, A.D., Garcia-Verdugo, J.M., Lim, D.A. & Alvarez-Buylla, A. (2003) Postnatal development of radial glia and the ventricular zone (VZ): a continuum of the neural stem cell compartment. *Cereb. Cortex.* **13**, 580–587.

Tropepe, V., Craig, C.G., Morshead, C.M. & van der Kooy, D. (1997) Transforming growth factor-alpha null and senescent mice show decreased neural progenitor cell proliferation in the forebrain subependyma. *J. Neurosci.* **17**, 7850–7859.

Viti, J., Gulacsi, A. & Lillien, L. (2003) Wnt regulation of progenitor maturation in the cortex depends on Shh or fibroblast growth factor 2. *J. Neurosci.* **23**, 5919–5927.

Wang, J. & Wynshaw-Boris, A. (2004) The canonical Wnt pathway in early mammalian embryogenesis and stem cell maintenance/differentiation. *Curr. Opin. Genet. Dev.* **14**, 533–539.

Warren, N., Caric, D., Pratt, T., *et al.* (1999) The transcription factor, Pax6, is required for cell proliferation and differentiation in the developing cerebral cortex. *Cereb. Cortex.* **9**, 627–635.

Warren, N. & Price, D.J. (1997) Roles of Pax-6 in murine diencephalic development. *Development* **124**, 1573–1582.

Yuasa, S., Kawamura, K., Kuwano, R. & Ono, K. (1996) Neuron-glia interrelations during migration of Purkinje cells in the mouse embryonic cerebellum. *Int. J. Dev. Neurosci.* **14**, 429–438.

Zigova, T., Pencea, V., Wiegand, S.J. & Luskin, M.B. (1998) Intraventricular administration of BDNF increase the number of newly generated neurons in the adult olfactory bulb. *Mol. Cell. Neurosci.* **11**, 234–245.

Zou, Y. (2004) Wnt signaling in axon guidance. *Trends Neurosci.* **27**, 528–532.

*Received*: 13 March 2005
*Accepted*: 11 July 2005

THE JOURNAL OF COMPARATIVE NEUROLOGY 483:329–340 (2005)

# Neuronal Generation, Migration, and Differentiation in the Mouse Hippocampal Primoridium as Revealed by Enhanced Green Fluorescent Protein Gene Transfer by Means of In Utero Electroporation

EIKO NAKAHIRA* AND SHIGEKI YUASA
Department of Ultrastructural Research, National Institute of Neuroscience, National Center of Neurology and Psychiatry, Kodaira, Tokyo 187-8502, Japan

ABSTRACT

Neuronal migration defects in the hippocampus during development are thought to be involved in various mental disorders. Studies of neural cell migration in the developing cerebrum have focused mainly on the neocortex, but those that have been performed on the developing hippocampal formation have not been adequately carried out. In the present study, the morphological differentiation of immature neurons that form the laminar structure of the hippocampus was investigated by labeling ventricular surface cells with the expression vector of the enhanced-green-fluorescent-protein (EGFP) gene. Vector DNA was transfected into spatially and temporally restricted neuroepithelium of the hippocampal primordium by in utero electroporation, and the morphology of EGFP-labeled migratory neurons and their interrelationships with the radial glial arrangement were observed. Pyramidal cells of Ammon's horn began to migrate radially along glial processes from a broad area of neuroepithelium on embryonic day (E)14. Large numbers of multipolar cells were found in the intermediate zone in the initial stage and stratified pyramidal cells appeared later. Dentate granule cells were labeled later than (E)16 and originated from a restricted area of neuroepithelium adjacent to the fimbria. Their initial migration was rapid and independent of radial glial fibers. Subsequent tangential migration in the subpial space and their ultimate settling into the forming dentate gyrus were closely associated with the radial glia. These findings indicate that distinct cellular mechanisms are involved in the development of the cortical layer of Ammon's horn and dentate gyrus. J. Comp. Neurol. 483:329–340, 2005. 

**Indexing terms: development; pyramidal cell; granule cell; radial glia**

The hippocampus contains the neural circuitry that is crucial for higher brain functions, such as learning, memory, and affect. Many pathological conditions, such as epilepsy (Houser, 1990; Lurton et al., 1997; Haas et al., 2002), lissencephaly (Sato et al., 2001; Ross et al., 2001), Down's syndrome (Raz et al., 1995), and psychiatric disorders (Benes and Berretta, 2001; Connor et al., 2004) are associated with histological abnormalities in the hippocampus, and the abnormalities are likely to be related to a disruption of neuronal migration during development. Thus, knowledge of neuronal migration during hippocampal histogenesis is necessary to be able to analyze the pathogenesis of the above conditions.

The development of cortical structures in the mammalian brain is achieved by a combination of two types of

Grant sponsor: Ministry of Health, Labor and Welfare, Japan; Grant number: Research Grant (15B-3) for Nervous and Mental Disorders (to S.Y.).

*Correspondence to: Eiko Nakahira, Department of Ultrastructural Research, National Institute of Neuroscience, National Center of Neurology and Psychiatry, 4-1-1 Ogawahigashi, Kodaira, Tokyo 187-8502, Japan. E-mail: nakahira@ncnp.go.jp

Received 19 August 2004; Revised 4 November 2004; Accepted 8 November 2004

DOI 10.1002/cne.20441

Published online in Wiley InterScience (www.interscience.wiley.com).